

AUTONOMOUS CRICKET BIOSENSORS FOR ACOUSTIC LOCALIZATION

A Thesis
Presented to
The Academic Faculty

by

Thomas Ian Mulcahey

In Partial Fulfillment
of the Requirements for the Degree
Master of Science in the
School of Mechanical Engineering

Georgia Institute of Technology
May 2010

Copyright © 2010 by Thomas Ian Mulcahey

AUTONOMOUS CRICKET BIOSENSORS FOR ACOUSTIC LOCALIZATION

Approved by:

Professor David L. Hu, Advisor
School of Mechanical Engineering
Georgia Institute of Technology

Professor Karim G. Sabra
School of Mechanical Engineering
Georgia Institute of Technology

Professor Marc W. Weissburg
Department of Biology
Georgia Institute of Technology

Date Approved: 2 April, 2010

ACKNOWLEDGEMENTS

To my advisor, Dr. David Hu, whose creativity inspired this project.

To Dr. Karim Sabra for providing endless knowledge, patience, and tutelage in the area of Acoustics.

To Dr. Marc Weissburg for providing the facilities to perform extracellular recording in, and for his patience in dealing with a mechanical engineer pretending to understand neurobiology.

To Tobi Horstmann, my intern from Germany during Summer 2009, without whom I could never have developed a working implant prototype.

To my family, my friends, and my girlfriend Brittany. I never would have made it through this process without their love, support, and encouragement.

Thank you to all involved in this project that made this work possible.

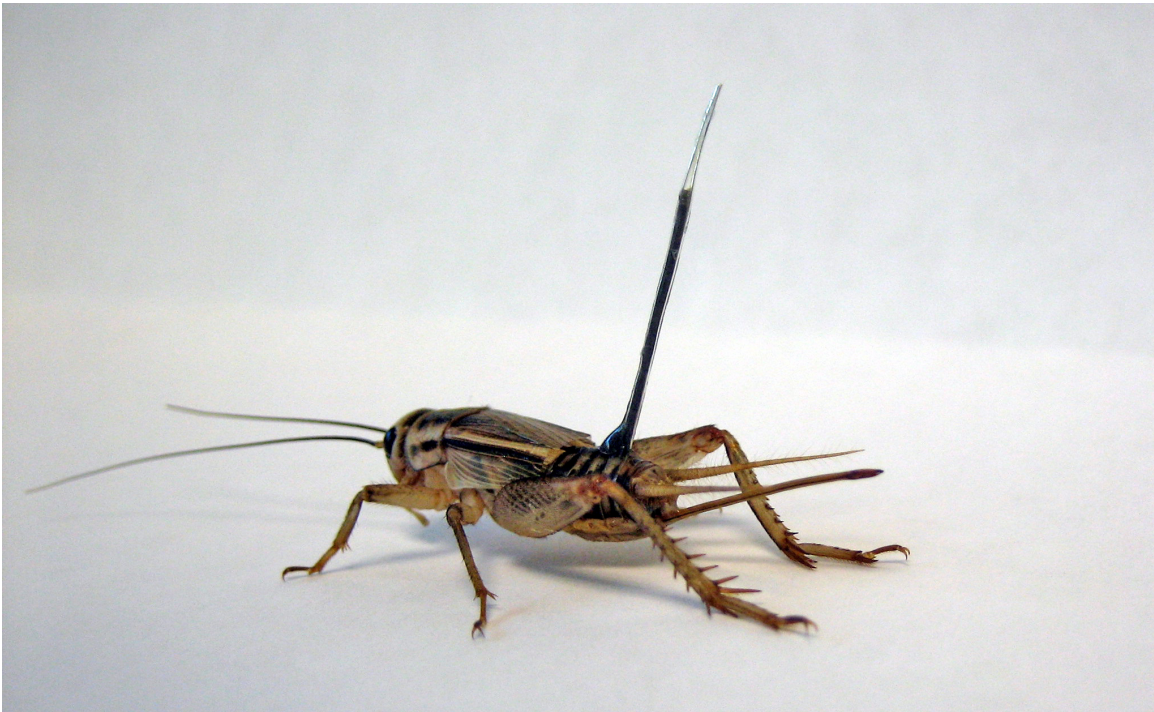


Figure 1: Cricket Acoustic Biosensor

TABLE OF CONTENTS

ACKNOWLEDGEMENTS	iii
LIST OF TABLES	vii
LIST OF FIGURES	viii
SUMMARY	x
I INTRODUCTION	1
1.1 Thesis Overview	2
1.2 Possible Applications	4
1.3 An Overview of Cricket Sensory Systems	6
1.4 Previous Research on Cricket Cerci	8
1.5 Cricket-Inspired Hearing Devices	9
II BEHAVIORAL RESPONSE TO SOUND AND VIBRATION	12
2.1 Background	12
2.2 Experimental Setup	13
2.3 Experimental Methodology	14
2.4 Results and Analysis	15
2.4.1 Response to Traveling Waves	17
2.4.2 Response to Standing Waves	18
2.4.3 Conclusions	18
III NEUROLOGICAL RESPONSE TESTING	20
3.1 Experimental Setup	21
3.2 Cricket Anatomy and Physiology	21
3.3 Multi-Unit vs. Single Unit Recording	23
3.4 Equipment	24
3.4.1 Acoustic Theory	24
3.5 Preparation Method for Extracellular Recording	28
3.6 Data Acquisition and Experimental Methods	29
3.7 Results	31
3.7.1 Response to Varied Center Frequency and Ramp Shape	33

3.7.2	Habituation Effect on Response	36
3.7.3	Cercal System Directional Sensitivity	37
3.7.4	Response to Background Noise	37
3.8	Discussion	39
IV	IMPLANT DEVELOPMENT	40
4.1	Implant Design	40
4.2	Surgical Procedure	41
4.2.1	Anesthesiology	42
4.3	Ventral Implantation	43
4.4	Dorsal Implantation	43
4.5	Implant Results	44
4.6	Discussion	46
V	CONCLUDING REMARKS	47
5.1	Future Work	48
APPENDIX A	WAVEGUIDE TESTING AND EXTRACELLULAR RECORDING METHOD- OLOGY	49
APPENDIX B	LABVIEW PROGRAMMING	58
APPENDIX C	RAW DATA	61
BIBLIOGRAPHY	63

LIST OF TABLES

1	Comparison of Auditory Frequency Ranges for a Few Animals [14]	1
2	Comparison of Cricket Cerci With Current Manmade Devices	5
3	Amplifier Settings	30
4	ANOCOVA Coefficients	35
5	ANOVA Coefficients	35
A.1	Saline Formulation	49
C.1	Raw Data: behavioral response to combined acoustic and vibration stimuli Table 1 of 2.	61
C.2	Raw Data: behavioral response to combined acoustic and vibration stimuli Table 2 of 2.	62

LIST OF FIGURES

1	Cricket Acoustic Biosensor	iv
2	Concept Sketch	5
3	Cricket Auditory Anatomy	7
4	Results Published By Previous Investigators	10
5	MEMS Biomimetic Cerci	11
6	Behavioral Response to Sound and Vibration Experimental Setup	13
7	Measured Behavioral Responses to Combined Excitation with Sound and Vibration For a Population of 20 Crickets	16
8	Results of 40 Hz Traveling Wave Testing	17
9	Results of 70 Hz Standing Wave Testing	18
10	Acoustic Response Testing Overview	22
11	Anatomy of the Cricket Cercal System	23
12	Design of Experimental Waveguide Setup	25
13	Dorsally Mounted Cricket Preparation With Hook Electrodes Under Ventral Nerve Cord	29
14	Example Acoustic Stimulus and Cricket Response	32
15	Total Spike Response as a Function of Center Frequency and Gaussian Standard Deviation	33
16	Analysis of Covariance (ANOCOVA) Model of Total Spike Response as a Function of Center Frequency and Gaussian Standard Deviation	34
17	Total Spike Response as a Function of Habituation to Repeated Stimulus	36
18	Normalized Directional Sensitivity as a Function of Gaussian Standard Deviation . .	38
19	Permanently Implantable Electrode Image	41
20	Schematic of Permanently Implantable Electrode Design	41
21	Robocricket	44
22	Signals Obtained from Robocricket Compared to Signals From Extracellular Recording	45
A.1	Spike Shapes Obtained Through Monophasic and Biphasic Recording	51
A.2	Waveguide Prototype 1 Validation	53
A.3	Waveguide Prototype 2 Validation	55
A.4	Block Diagram of DAQ Programming	56

A.5	Cricket Response to Bandpass Filtered White Noise	57
B.1	Labview program for reading a single stimulus WAV file and recording cricket response	58
B.2	Block Diagram 1 of 2 for reading and playing multiple WAV files, recording cricket response, and resolving spike temporal locations	59
B.3	Block Diagram 2 of 2 for reading and playing multiple WAV files, recording cricket response, and resolving spike temporal locations	60

SUMMARY

The goal of this project was to design networked arrays of cricket biosensors capable of localizing sources such as footsteps within dangerous environments, with a possible application to earthquake detection. We utilize the crickets natural ability to localize low frequency (5 Hz – 600 Hz) acoustic sources using hair-covered appendages called cerci. Whereas previous investigations explored crickets neurological response to near field flows generated by single frequency steady-state sounds, we investigated the effects of transient waveforms, which better represent real world stimuli, and to which the cercal system appears to be most reactive. Extracellular recording electrodes are permanently implanted into a crickets ventral nerve cord to record the action potentials emanating from the cerci. In order to calibrate this system, we attempt to find the relationships between the frequency and direction of acoustic stimuli and the neurological responses known as spike trains, which they elicit. The degree of habituation to repeated signals that exists in most neurological systems was also experimentally measured. We process the signals to estimate frequency and directionality of near field acoustic sources. The design goal is a bionic cricket-computer system design capable of localizing low frequency near field acoustic signals while going about its natural activities such as locomotion.

CHAPTER I

INTRODUCTION

Crickets possess one of the keenest acoustic detection systems in the animal kingdom. Through the combined use of three sensory mechanisms, a total sensitivity range of 5 Hz to greater than 100 kHz [19] is achieved, 20 times broader than the human perception range of 20 Hz - 20 kHz [4]. In addition to having a broad frequency perception, crickets are capable of detecting dynamic airborne disturbances as low as 2 mm/s [24]. Such small disturbances may be caused by the wingbeats of a wasp from a distance of 9 meters. Their hearing abilities are truly extraordinary.

High sensitivity is accomplished by specialized appendages called cerci, covered in hundreds of hairs sensitive to air particle motion. The field of biomimetics aims to design novel devices inspired by natural biological systems, since millions of years of evolution have yielded what many consider to be optimal designs. The field of biosensor design takes the idea of biomimetics one step further, by coupling the biological system to traditional sensor circuitry, eliminating the need to fabricate a sensor. The goal of this project was to utilize the natural low frequency sensitivity of the common house cricket *Acheta domesticus* to develop a biosensor capable of detecting and localizing near-field acoustic signals with a theoretical directional accuracy between 4.7° and 7.7° [43]. While a complete, autonomous system was not developed, information about the ways crickets

Table 1: Comparison of Auditory Frequency Ranges for a Few Animals [14]

Animal	Lowest Detectable Frequency	Highest Detectable Frequency
Humans	20 Hz	20,000 Hz
Dogs	40 Hz	60,000 Hz
Mice	1,000 Hz	90,000 Hz
Bats	20 Hz	120,000 Hz
Dolphins	250 Hz	125,000 Hz
Crickets	5Hz	> 100,000 Hz

encode certain features of sound stimuli was gleaned, which could allow for the calibration of such a system.

1.1 Thesis Overview

In order to determine the optimal use of the cricket as a biosensor, work was broken down into three phases:

- Verification of behavioral responses to simultaneous acoustic and vibratory stimuli is presented in Chapter 2.
- In Chapter 3 we discuss a method of measuring and decoding the neural signal in the ventral nerve cord and measurement of directional sensitivity of cricket cerci.
- Development of an electrode and a method of permanent implantation and measurement is presented in Chapter 4, a step required to allow for full sensor autonomy.

The long term goal of this project was to determine the feasibility of semi-artificial cricket biosensors capable of detecting the directionality and frequency content of low frequency acoustic fields. The subject under investigation was *Acheta domestica*, the common house cricket. Cricket cerci transduce airborne acoustic waves to electrical neurological signals, which we investigated. Crickets possess an extraordinary ability to detect signals down to the infrasonic frequency range, and localize them with astonishing accuracy within the near field of the source of excitation. Current acoustic testing methods require sensors located in the far field of the source to be accurate, which can require on the order of 35 meters for infrasonic frequencies, showing a distinct advantage of this type of sensor.

A series of experiments were designed to verify prior assumptions regarding cricket locomotion in response to combined airborne sounds and substrate vibrations. Previous investigators showed that crickets move away from a low frequency sound source, a behavior termed negative phonotaxis. We studied motion of crickets placed on a steel plate coupled with a sound source at one end. Harmonic acoustic excitations were generated. Substrate vibrations induced by the acoustic field were measured using a laser doppler velocimeter. The results of this testing verified that as long as the substrate vibrations could be classified as traveling waves, the cricket responded with negative

phonotaxis. In the case of standing waves, the cricket was tricked into moving toward the sound source, violating the previously accepted negative phonotaxis assumption. Further analysis of the data and direct observation showed that crickets prefer to move along paths of minimal surface velocity when presented with the opportunity, even if such paths lead toward the sound source.

Extracellular recording techniques were used to measure neural activity in the cricket’s ventral nerve cord resulting from acoustic stimuli. A cylindrical waveguide with phased drivers at each end was fabricated to provide low frequency acoustic plane waves for stimulation. Stimulus signals used were both sinusoidal and white noise waveforms, each modulated by Gaussian functions. To characterize the neurological response to the effects of center frequency, the attack of the stimulus, or ramp time, controlled by varying Gaussian standard deviation, stimulus direction with respect to the animal, and habituation to repeated signals were isolated. The directional sensitivity was plotted and compared to the results reported by previous researchers, with maximum sensitivity to stimuli originating directly behind the cricket. It was also shown that response was maximized, in terms of total action potentials, by providing impulsive stimuli with low Gaussian standard deviation. It was determined that response in the ventral nerve cord is not a function of the center frequency used, but only of the shape of the bounding function. This relationship makes intuitive sense since the predatory stimuli that the cerci are designed to react to are typically impulsive sounds like footsteps, which require quick reactions. Stimuli with long ramping times may not correlate to any threatening signals that occur naturally, and therefore the response is minimized within the cercal system. Since our experimental results indicate sensitivity only to transient portions of stimuli, the cricket is best suited as a vector sensor to detect dynamic changes to the surrounding acoustic field.

Finally, an implantation methodology was developed to permanently implant an extracellular electrode in the cricket abdomen. A dual hook silver electrode coated with Teflon was designed and fabricated. A surgical method to implant the electrode was developed using multiple techniques and anesthesia methods. After numerous implantation techniques were developed using mechanical manipulators, it was determined that the optimized method was to design a holding mechanism for the animal and to implant manually under a microscope. The resulting implanted cricket had dorsally protruding extracellular leads which were connected to the amplifier via modified clips.

This wired version was tested and compared to standard extracellular techniques. While response from the implant had a lower signal to noise ratio and decreased sensitivity, the testing proved that signals could be measured from a live specimen, which was able to survive for up to 6 days with current methods. Development of a miniature wireless transmitter, battery, and miniature amplifier by future investigators could lead to effective application of the cricket as an autonomous biosensor.

Once all phases were completed, the results obtained from each were compiled to examine the feasibility of the cricket as a biosensor. We determined that with current technology, and the complexity of such a device, that the use of this biosensor for acoustic measurement is impractical at this time. While the cricket provides substantial information processing, the signals measured from the cercal system require much more analysis to gain useful information, which is an undesirable trait for an effective sensor.

1.2 Possible Applications

Current acoustic measurement devices typically require the transducer to be placed in the far field of the source for measurements to be accurate and meaningful. For example, localization of a 5 Hz signal, such as that produced by an earthquake, requires sensor spacing up to 35 meters, about $1/2$ wavelength to meet this criteria. Instead, use of a cricket biosensor eliminates the far field requirement, as the cricket's cercal system gathers information about the complicated near field in order to resolve information about the source location and frequency content.

This technology may be used for a number of applications involving low frequency measurement. One such application is the early detection of earthquakes. Earthquakes emit a p-wave, which propagates much faster than the subsequent s-waves that can cause catastrophic surface damage to structures. P-waves are difficult to detect and localize due to their infrasonic frequency content, less than 20 Hz. In the best case scenario, a cricket sensor system located far from the epicenter of an earthquake could provide up to a minute of advanced warning. This could provide sufficient time for people to vacate their dwellings and find a safe hiding place, or for an automated building suspension system to adjust its stiffness, reducing potential damage.

Table 2: Comparison of Cricket Cerci With Current Manmade Devices

	Crickets	Man Made Devices
Lowest Frequency Detectable	5 Hz	5 Hz - but requires microphones about 30 meters apart ($\lambda=64\text{m}$)
Detection in Noisy Environments	Detect very quiet signals in loud spaces	Increased background noise increases signal processing difficulty
Signal Processing	Embedded	Requires significant processing power and complexity

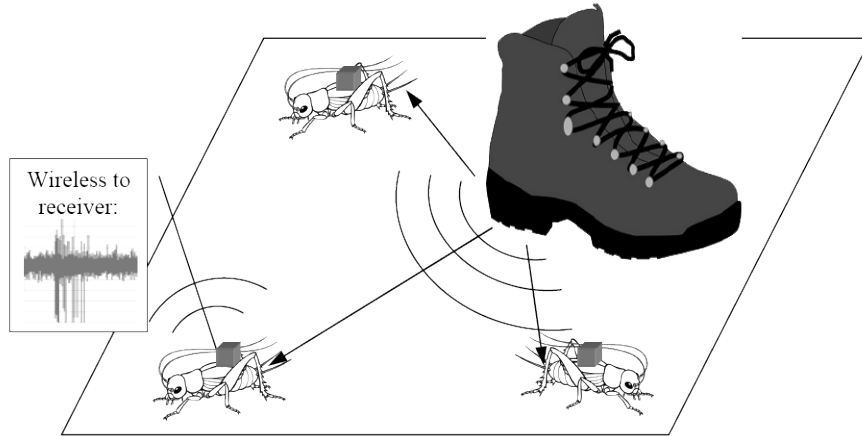


Figure 2: Concept sketch indicating biosensor application to detection of footsteps. Multiple crickets are implanted with electrodes, which wirelessly transmit data to a central processing computer, which reduces the data to cricket location and orientation, the vector direction to the source, and the frequency content of the source. Combining data from multiple crickets allows for triangulation

1.3 An Overview of Cricket Sensory Systems

The cricket’s extraordinary sensing ability stems from its survival instincts. Each of the three sensory systems shown in Figure 3 is responsible for performing a specific task, related either to mating or escape from predators. The cricket’s low frequency sensitivity, in the range of 5 Hz - 600 Hz is facilitated by the cercal system. The cerci are two 1 cm long conical appendages protruding from the rear of the cricket, covered in thousands of hairs up to 3 mm long, which gather information about the surrounding fluid field. The cerci are shown in Figure 3d. Information from the individual hairs on the cerci is combined in the terminal abdominal ganglia (TAG), which encodes the information in a series of action potentials that then propagate up the ventral nerve cord. The cercal system has evolved to help crickets escape from predators approaching from the rear, where typically visual cues are unavailable. The low frequency fields that excite the cerci through viscous forces resulting from air particle oscillation are associated with the approach of ground of aerial predators [19]. The system triggers an escape response to the cricket, resulting in a kick from the powerful hind legs, followed by locomotion in a direction opposite the source.

Tympanal membranes located on the knees of the forelegs, connected through a series of waveguides, are responsible for the transduction of acoustic pressure. The intermediate range of this system is used to detect and localize mating sounds from stridulating crickets [19]. The need for sensitivity to signals as high as 100 kHz is related to predatory response to bats, which use ultrasonic chirps for echolocation in order to navigate while in flight.

The subgenual organs are located in each of the cricket’s forelegs. These organs are responsible for the detection and transduction substrate vibrations. Acting as inertial masses inside the hollow leg cavities, the organs operate similar to an accelerometer. The motion of the leg caused by surface vibration causes a relative motion between the subgenual organ and the exoskeleton of the leg. This relative motion is sensed by the connectives to the organ as shown in Figure 3c. This information propagates to the omega interneuron [46] where information from the subgenual organs is compared with the signals propagating from the cerci. The omega interneuron acts as a comparator that determines which signal is more relevant at the time, and allows that signal to continue up the ventral nerve cord to the brain.

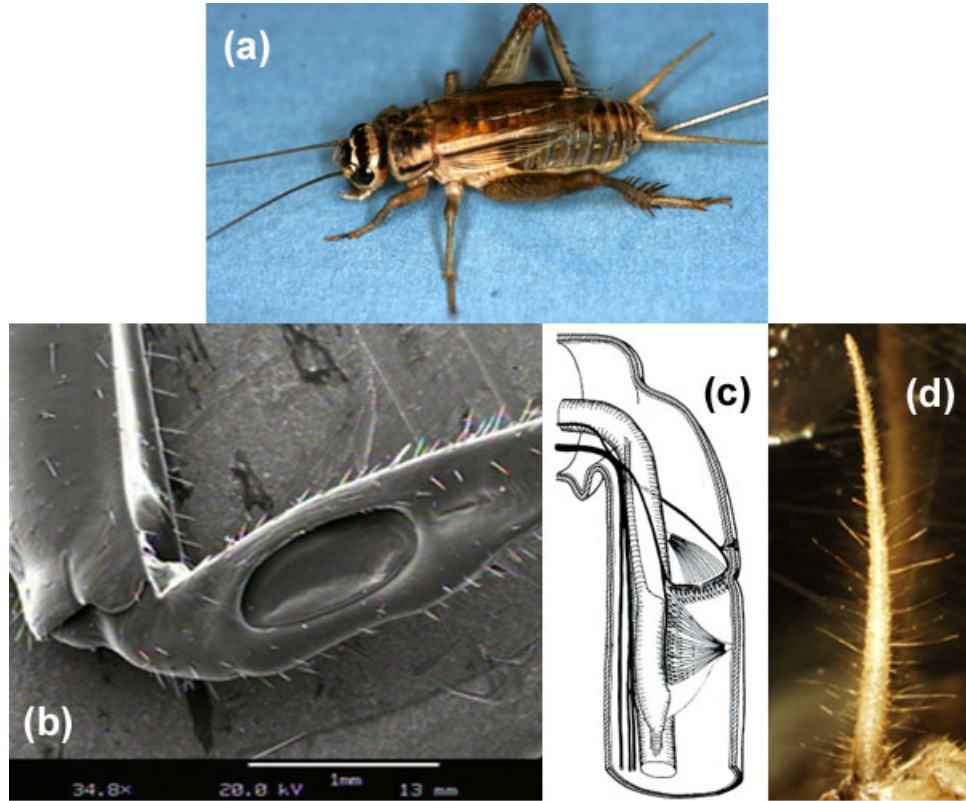


Figure 3: Cricket Auditory Anatomy. **a.** *Acheta domestica* **b.** Tympanal Membrane (Reproduced Courtesy Huber,1989 [19]) located just below the knees of the lower forelegs. This organ is used to sense sounds in the range of 500Hz to 100kHz **c.** Subgenual Organ [19] located in the lower forelegs, used to sense substrate vibration **d.** A cercus showing the hundreds of filiform hairs used to sense low frequency air particle motion.

1.4 Previous Research on Cricket Cerci

Of all the cricket’s auditory systems, the cerci are best understood. Sufficient previous experimental work has been done to characterize the motion of cricket and other arthropod hairs excited by oscillatory flows [7, 15, 17] and by touch [6]. Each cercus is equipped with approximately 400 filiform hairs [28, 5] sensitive to a number of stimuli including tactile contact, acoustic signals, and variations in the direction of flow in a fluid medium. The hairs range from 50 μm to 1.5mm in length with diameter on the order of 3-5 μm [5]. Dangles *et. al* studied wild populations of crickets and categorized the cercal hair canopies of many species according to the developmental instars. Other researchers [30] studied on the robustness of cerci, as shown by and the cricket’s ability to regenerate cercal hairs and even whole appendages.

Concomitant fluid dynamic modelling (viscous) has been done by numerous groups [41, 20, 18] to predict the motion of the hair canopy in response to acoustic flows.

Dijkstra[7] reports the following spring constant K_θ and effective damping constant R for a 200 μm long hair resulting from the viscoelasticity of the socket material: $K_\theta \approx 10^{-12}$ N m s/rad, the moment of inertia of the hair about the base socket is $J \approx 5 \times 10^{-21}$ kg m², $R \approx 10^{-16}$ N m s/rad. These researchers have concluded that impedance matching between the torsional resistance and the drag resistance on the hair has led to maximum energy transfer from the fluid medium to the mechanosensory system, allowing for optimized sensitivity to air particle oscillation [15, 41].

Furthermore, the hairs are so lightweight that background noise can actually improve the hair’s sensitivity to extremely small variations in flow through a mechanism known as stochastic resonance [27]. By adding background noise, the signal-to-noise ratio present is increased resulting in sensitivity to air currents as low as 2mm/s, on the order of the magnitude of a digger wasp wingbeat from 9m [19]. Stochastic resonance has been shown in man-made sensor systems [33, 44] to play a part in detecting signals that would not be detectable by a single sensor.

A number of publications are available that describe the neurological activity of the cercal system [41, 22], as well as the physiology involved in the transduction process [11, 2]. **A common method used in this research is to count the total number of spikes, or action potentials, that take place in response to a single acoustic stimulus.** This method has resulted in agreement among researchers regarding directional sensitivity of the cercal system, with the highest response

elicited from directly behind the cricket, and the lowest from directly in front. The results on directionality summarized by Jacobs [22] are reproduced in Figure 4a. In Figure 18 we have confirmed this relationship.

Jacobs[22] and Kämper[24] also use this method of counting the total number of action potentials that occur during the course of a stimulus. In their tests they determine the cercal system’s response to low frequency acoustic stimuli as a function of frequency using an acoustic wind tunnel. In order to isolate discrete frequencies, they modulated sinusoidal signals with long amplitude ramps, eliminating transient effects. Additionally, they varied their ramp shape for each frequency of interest, which does not isolate the frequency contribution to response as they intended. The resulting publications of this work suggest that there is **no correlation** between the total action potential count and center frequency in the cercal system, evidenced by the exhibit reproduced in Figure 4b.

Our research aims to prove that the frequency content of the signal does have an effect on the overall spike production in the ventral nerve cord. Kämper presents the case that frequency may be encoded by a more sophisticated mechanism. In this study we investigated spatiotemporal encoding of signals among neurons, which will be discussed further in Chapter 3. A few groups have attempted to prove that this information *must* be encoded by the cercal system through the use of information theory developed by Shannon [3, 8, 16, 40] which model the cercal system as a communication channel.

Other researchers have taken a neurophysiology approach to studying the cercal system. Some groups [31, 41] have attempted to map the locations in the Terminal Abdominal Ganglion that correspond to frequency and directionality content of stimuli, while others [10, 29] have attempted to model the ion channels that carry signals in order to essentially determine the “wiring diagram” within the cercal system.

1.5 Cricket-Inspired Hearing Devices

This project was motivated by a group called the CiCADA Project [7, 21, 23], which has been developing a MEMS device designed to mimic cricket cerci. While they have been successful in developing a transducer capable of coupling with acoustic fields, they have yet to develop signal

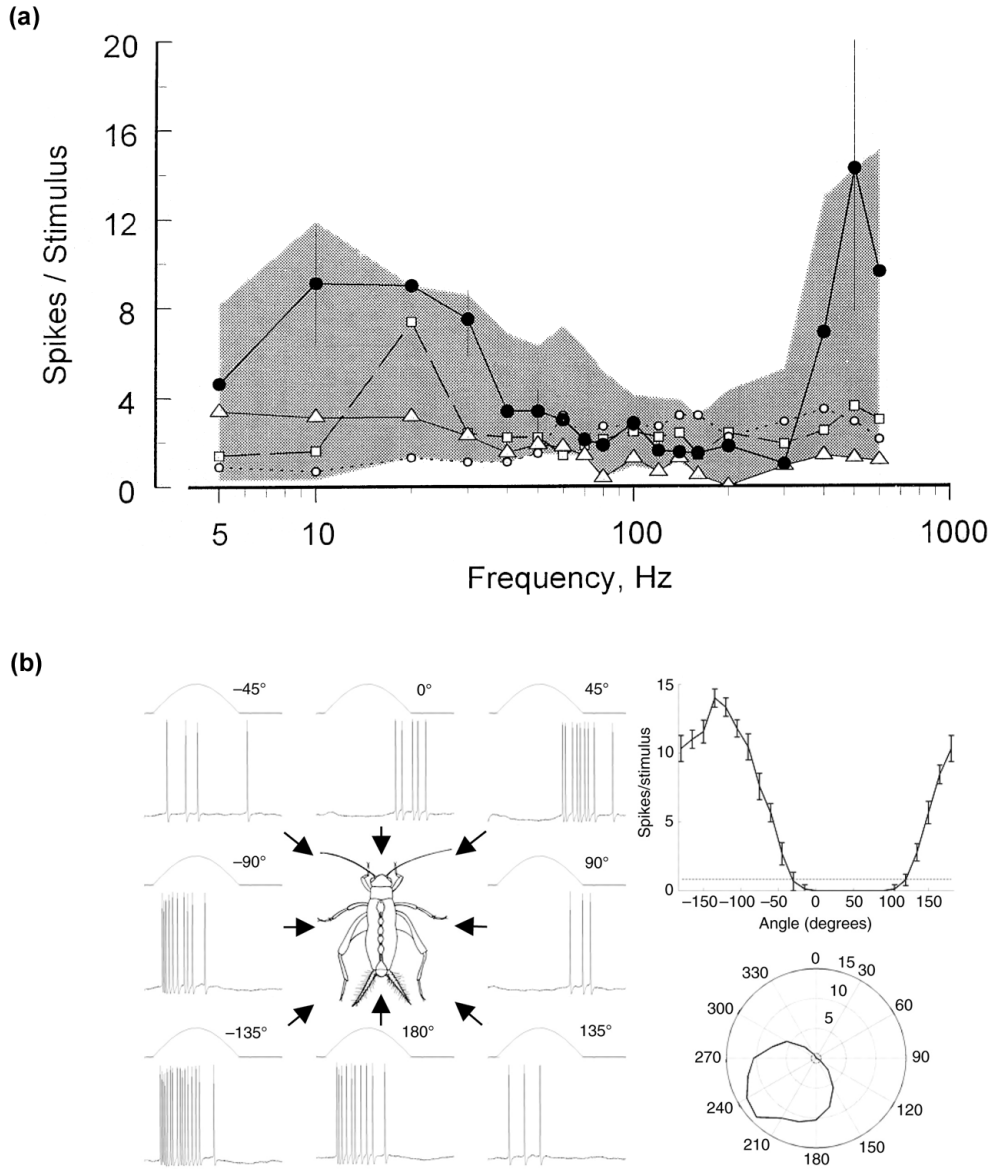


Figure 4: Results published by previous investigators. **a.** Total spike count as a function of stimulus frequency [24]. Each trace presented represents a measurement at a different interneuron. The dark area surrounding the data is an error cloud. **b.** Total spike count as a function of stimulus direction [22]. Left: sample electrophysiology measurements. Right Top: linearly scaled response to stimulus as a function of direction. Error bars represent standard deviation for measurements. Right Bottom: polar plot of directional sensitivity. Radial axis represents the total number of spikes measured.

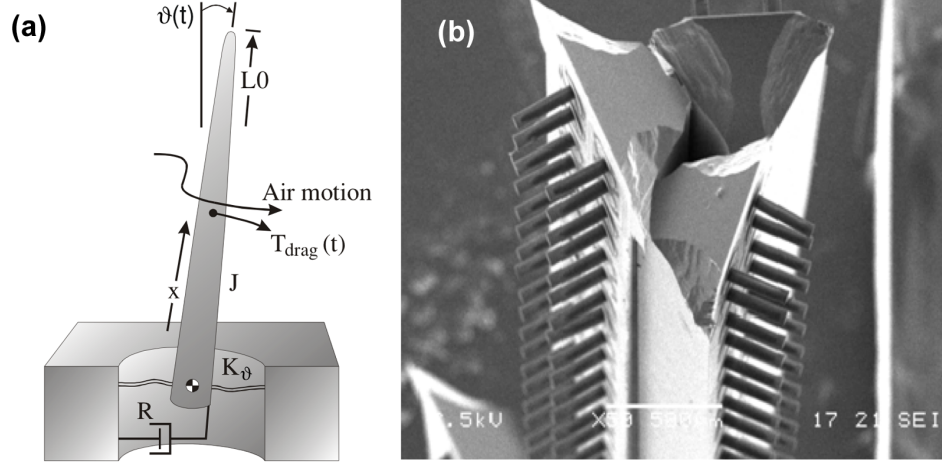


Figure 5: MEMS biomimetic cerci developed by CiCADA group, University of Twente. **a.** Fluid dynamic model used to predict frequency response to fluid oscillation [7, 23] **b.** SEM of MEMS biomimetic cerci [21]

processing techniques in order to convert the hundreds of signals obtained from individual hairs into an overall ensemble response which gives information about the properties of the fluid field.

The novelty of this project is the use of the cricket itself as a transducer, making use of the advanced signal processing provided by the Terminal Abdominal Ganglion (TAG). By decoding the signals already present in the cricket's ventral nerve cord, the process of fabricating a transducer is avoided. In addition the animal provides the majority of the processing required to gain useful data from hundreds of mechanosensory hairs, simplifying the amount of computation required to decode the signals.

CHAPTER II

BEHAVIORAL RESPONSE TO SOUND AND VIBRATION

2.1 Background

Studies into the behavioral response of the cricket date back to the 1970's. Generally these studies have focused on the escape response elicited by low frequency acoustic sounds and low frequency acoustic flows. Low frequency stimuli are thought to mimic signals resulting from the locomotion of predators through movements such as wingbeats by flying predators or footsteps by terrestrial predators [19]. Until now it has been accepted that crickets respond through negative phonotaxis [19, 1], implying that the animal senses the direction from which the stimulus emanated and responds with locomotion in the opposite direction. Most of these tests attempted to isolate the sound stimulus in order to eliminate any other sources of excitation such as surface vibrations caused by coupling with the acoustic waves.

The most comprehensive testing that has been done to date, reported by Huber *et al.* involved the use of a tracking ball on which the cricket was tethered in an enclosed, darkened environment. A small speaker was used to excite the cricket and resulting motion was measured and recorded. This testing categorized motion in response to both low frequency sounds which excite the cerci, and intermediate frequency (4-6 kHz) signals associated with cricket mating calls. Results of this testing showed that crickets associate low frequency sounds with predatory advances. This conclusion was based on the observations that a singing cricket would stop singing when presented with this stimulus and assume a defensive position. In addition the cricket would proceed to exhibit negative phonotaxis in response to repeated exposure to these stimuli. Huber noted the opposite effect when the cricket was presented with the intermediate frequency tones. Crickets associated these sounds with mating signals and unlike the previous testing, exhibited positive phonotaxis.

Other researchers such as Wiese [46] performed neurophysiological recordings in a location of the ventral nerve cord called the Omega Interneuron. This research used intracellular recording to determine the signals in the nerve cord resulting from acoustic signals alone, vibration signals

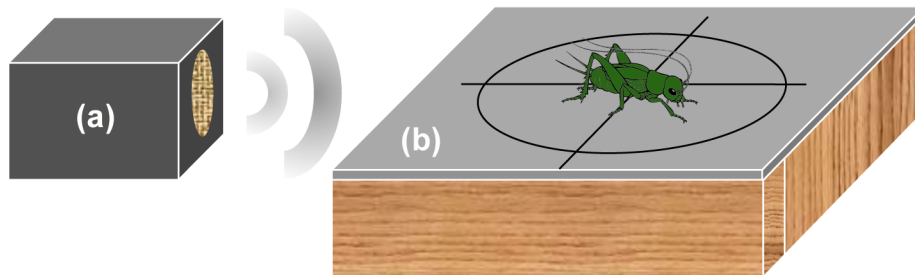


Figure 6: Behavioral response to sound and vibration experimental setup. **a.** Subwoofer **b.** Wave Plate

alone, and combined acoustic and vibration stimuli. While this work did not include any behavioral observation in response to combined stimuli, the neurophysiology did reveal that the resulting neurological “spike train” was a function of the relative levels of each form of excitation.

It was our opinion that the more interesting data would come from the crickets behavioral response when presented with both vibratory and acoustic stimuli simultaneously. In most real world scenarios there is a distinct relationship between acoustic fields and the ground vibrations with which they couple, and rarely does one mode of excitation exist without the other [13].

2.2 *Experimental Setup*

In order to determine the cricket’s response to simultaneous acoustic and vibratory stimuli, an experimental setup was constructed consisting of a wave plate, a small cylindrical enclosure to contain the cricket in the center of the plate until testing began, a loudspeaker, and a computer to generate sinusoidal tones. The resulting experimental setup is shown in Figure 6. The wave plate was designed to accommodate both standing waves and traveling waves within the range of frequencies under investigation.

The so-called “wave plate” was fabricated from 24 gauge (approximately 0.7mm thick) galvanized sheet steel. A 24 inch square was cut from the material onto which a 20 inch compass was drawn on the steel with 10° increments to use as reference for the orientation of the cricket before and after the stimulus was administered.

The plate was framed using douglas fir timber (1.5 inches by 3.5 inches) and fastened to the frame using sheet metal screws spaced 1.5 inches apart. This configuration allowed the plate to be modeled

approximately as a free plate with clamped edge boundary conditions, for which modes of vibration as well as natural resonances could easily be predicted with acceptable accuracy using known equations [47]. In order to determine whether the motion of the wave plate was best characterized by a traveling wave or a standing wave, a Polytec[®] scanning laser doppler velocimeter, or LDV, was used to map the velocity field of the plate surface in response to each of the harmonic test frequencies of interest. The velocity field was then represented as a three dimensional isometric view. If a clear node line existed, the motion was categorized as standing wave motion.

Low frequency signals as low as 20 Hz were generated using the Acoustimass[™] module from a Bose[®] Companion 3[™] system. The module utilized a 6.5" driver along with a proprietary waveguide system to develop clear low frequency signals with limited distortion. Sound levels were calibrated using a 1/2 inch Larson-Davis Model 2541 condenser microphone with a 2200C preamplifier. LabVIEW[™] software was used to convert the transducer's signals into decibel (dB) levels using internal Virtual Instruments (VI's) created for sound level measurement. The sound level used for testing was approximately 85 dB re20 μ Pa

2.3 Experimental Methodology

All experiments were performed in the dark with carpeted floor and sheet-rock walls to minimize reflections of the acoustic source, maintaining some of low frequency directionality. Background noise was minimized to a floor level of around 50 dB SPL, tested using a Larson-Davis sound level meter. Each cricket studied was examined prior to testing to determine if any defects existed in the cerci such as bent, broken, or missing hairs or even missing portions of a cercus. Only unmarred specimens were tested. An individual specimen was placed in the center of the wave plate and covered with an 8 ounce glass until the cricket stopped exploring the space and picked a static initial orientation. The orientation of the cricket was recorded, referenced by the compass which was drawn on the surface. The compass was marked on one side from 0 to 180°, with 0° corresponding to an orientation directed from the center toward the speaker. The other side was indicated as 0 to -180° to indicate that the cricket turned in the opposite direction. A measurement of $\pm 180^\circ$ indicated that the cricket exhibited negative phonotaxis. Response was measured for signals consisting of single tones from 40 Hz to 240 Hz in 30 Hz increments. At

least 30 seconds was allowed between trials for the animal to once again become comfortable with its environment. Each specimen was tested for two trials through the full frequency range, at which time they would return to the enclosure with the other crickets. A new test subject was then used for subsequent testing. This methodology provided a response which was not subject to habituation due to repeated exposure to similar signals. Behavioral response was measured for 20 different specimens providing a sample population of $n = 20$. A total of 40 data points for each stimulus frequency was recorded and analyzed.

2.4 Results and Analysis

The information for the 40 data points taken at each stimulus frequency from 20 different crickets was compiled and plotted in histogram format. The bin sizes were chosen in 10° increments to display the data with the same angular resolution with which the data was taken. The following sections include histograms which represent the most common responses to traveling and standing waves. Raw data sets can be found in Appendix C. Figure 7 presents a statistical summary of the responses recorded. Circular statistics was performed in Matlab using the Circular Statistics Toolbox developed by Berens and Velasco.

Data was separated according to the type of surface vibration observed. LDV measurement was used to categorize surface vibrations as either standing waves, which are common in plates excited at or near resonance frequencies, or traveling waves that occur when excitation is in between plate modes. Data analysis shows that when surface vibration is standing, crickets escape at an angle less than 90 degrees with respect to the source. In the case of traveling waves, crickets repeatably escape at angles greater than 90 degrees. Resultant vectors were calculated for the circular data sets that show the mean behavioral response for each excitation frequency. Standing and traveling wave classifications are represented in Figure 7a by data markers. The horizontal line $y = 90^\circ$ makes the distinction between travel toward the sound source ($< 90^\circ$) and escape in a direction opposite the sound source. It should be noted that all standing wave frequencies result in escape in the direction of the sound source.

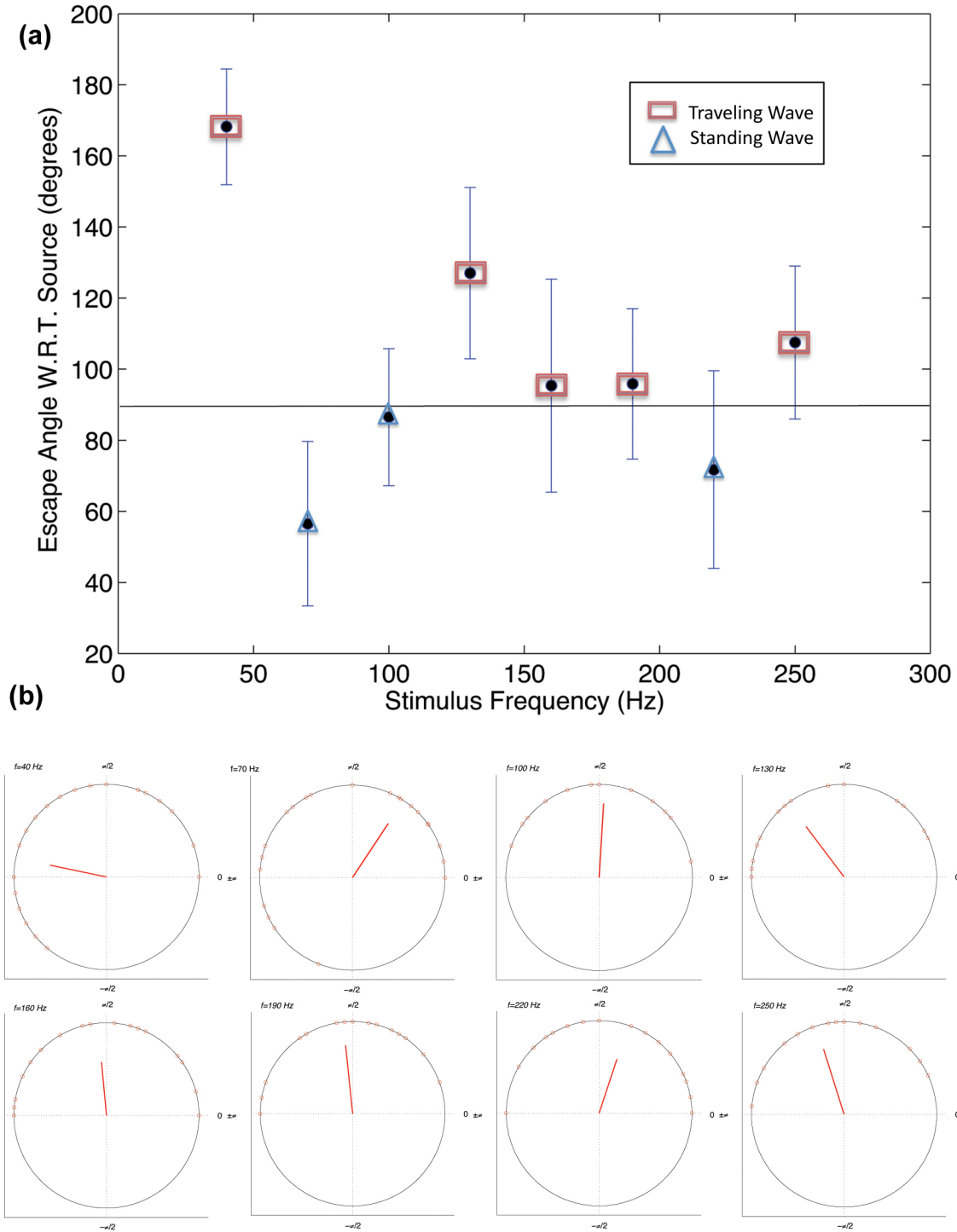


Figure 7: Measured behavioral responses to combined excitation with sound and vibration for a population of 20 crickets. **a.** Box and whisker plot of mean observed responses by excitation frequency. **b.** Results of circular statistical analysis. Red lines represent resultant vectors while red circles represent individual data points.

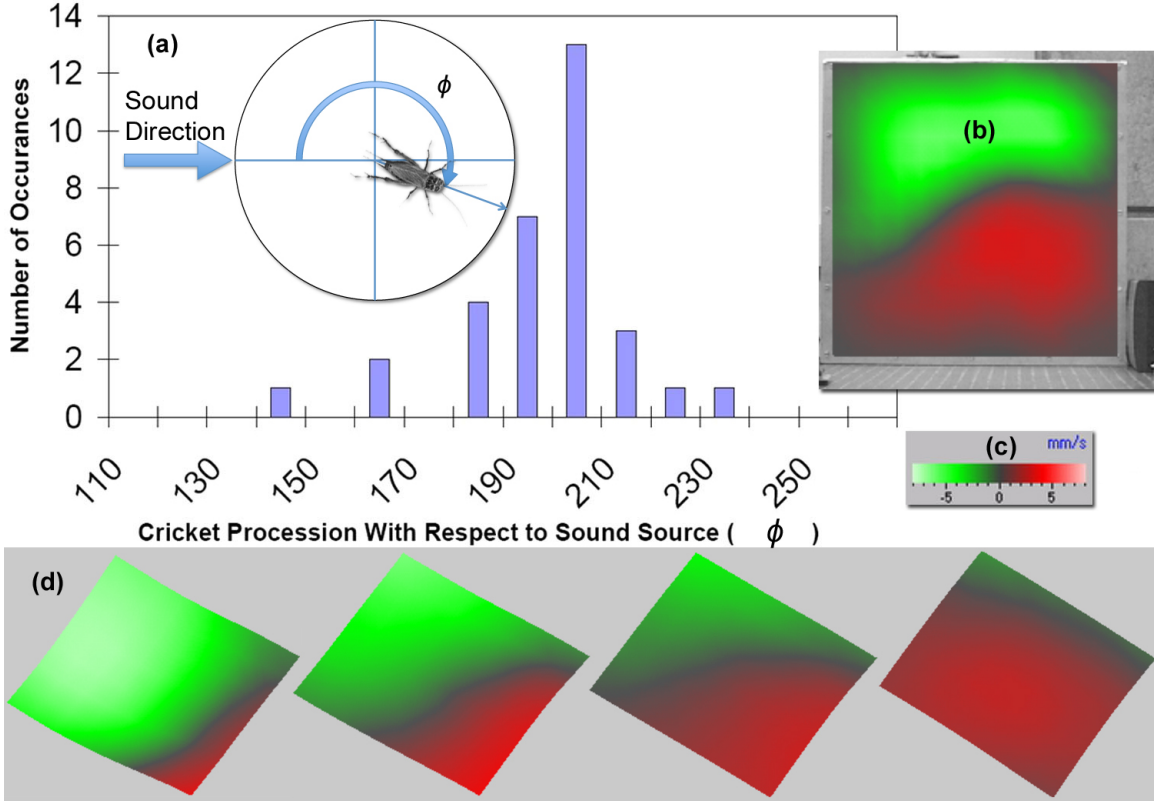


Figure 8: Results of 40 Hz traveling wave testing. **a.** Histogram of cricket locomotion in relation to the origin of acoustic stimulus with concentration around 210°. Corresponding orientation is indicated on the inset cartoon. **b.** Image of measurement setup during LDV testing, note the orientation of the subwoofer in the bottom right hand corner of the plate. **c.** LDV Velocity Legend **d.** 4 sequential isometric frames during one cycle of the LDV map of plate surface corresponding to a 40 Hz acoustic stimulus. The dark line in each image indicates the node of a traveling wavefront.

2.4.1 Response to Traveling Waves

Traveling waves correspond best with ground motion that would most likely occur in nature. Figure 8 shows a typical behavioral response distribution to this type of excitation. The data exhibited was collected using a 40 Hz pure sinusoidal stimulus.

Figure 8b-d shows the LDV representation of the surface velocity of the plate. The black area represents the starting node line, or line of zero velocity, which moves across the plate with time. This indicates a traveling wave across the plate. In a standing wave, the nodal line would be temporally stationary. As shown in the histogram, the crickets studied had a clear tendency to travel at about 200° with respect to the source. This corresponds to negative phonotaxis, in accordance with the data presented by previous investigators.

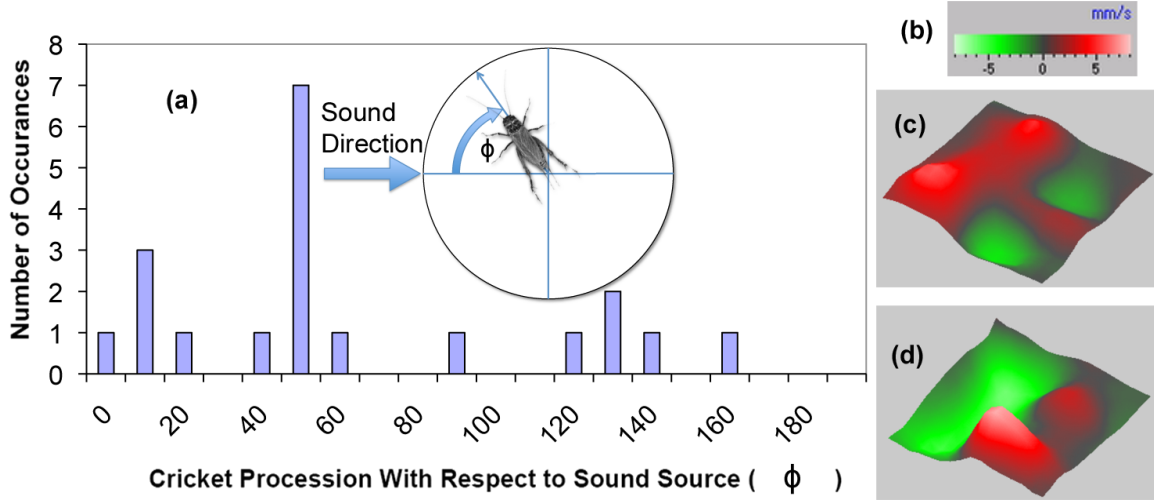


Figure 9: Results of 70 Hz standing wave testing. **a.** Histogram of cricket locomotion in relation to the origin of acoustic stimulus **b.** LDV Legend **c.-d.** LDV map of plate surface corresponding to a 70 Hz acoustic stimulus at two different times in a cycle. The same LDV setup was used as presented in Figure 8b. Two frames were used since this symmetric pattern repeats every other frame.

2.4.2 Response to Standing Waves

Standing waves are characterized by an LDV map which indicates a stationary node line. Finite boundaries are required to create internal reflections that lead to the additive interference among waves within the material that create standing wave patterns. Figure 9b shows that the wave plate exhibits this characteristic motion in response to a 70 Hz acoustic excitation.

A clear difference exists between the histograms presented in Figures 8 and 9. The subjects exhibited a tendency to move in an orientation approximately 50° with respect to the source. This motion actually suggests positive phonotaxis at first glance. Further analysis of the LDV map indicated that the cricket was actually traveling along the nodal line of zero vibration. This type of response was also characteristic of the remaining standing wave frequencies, correlating to motion along minimal vibration equipotentials.

2.4.3 Conclusions

When presented with a stimulus consisting of both an acoustic signal and a vibrating substrate, crickets naturally exhibit negative phonotaxis to acoustic stimuli which exceed the threshold limit unless a path of minimal vibration exists, such as the case of the standing wave. This result is important because previous research indicated that cercal response alone was responsible for

the negative phonotactic behavior. This research effort was the first time both stimuli have been presented simultaneously, determining that vibration response from the subgenual organs takes precedence over the information received from the cerci. This is important in terms of an engineering system because if it was desired that a cricket biosensor was to convey information about both substrate vibration and the acoustic field, it would not be possible to measure both from the ventral nerve cord with a single neural recording, as the information about vibration would clearly take precedence over the acoustic information conveyed by the cerci.

CHAPTER III

NEUROLOGICAL RESPONSE TESTING

Using traditional methods of electrophysiological recording, we attempted to utilize the cricket as a biosensor to detect low frequency acoustic fields. The generalized concept consists of an array of crickets equipped with extracellular recording devices which could transmit signals emanating from the cercal system of the house cricket *Acheta domesticus* to a remote computer station to be decoded. The goals of the decoding process were to extract information about the directionality of the stimulus in relation to the animal's orientation as well as the frequency content of the signal. In order to facilitate this decoding process, the cricket sensor had to first be calibrated using acoustic stimuli with well quantified characteristics.

Previous researchers have long been aware of the cercal system's ability to encode directionality information regarding the origin of dynamic air stimuli [19, 22], which has typically been presented in the form of a total number of neurological action potentials per stimulus. Many of these researchers additionally attempted to determine whether or not a neural representation of the frequency content of the stimulus signal was also present, but were unable to determine clear relationships. Kämper stated at the end of his (1998) paper that "Frequency information is most likely filtered from the neural signal in the TAG, and may be difficult to find using traditional means" The purpose of this portion of our research aimed to elucidate the mechanisms with which the cercal system encodes frequency information about acoustic stimuli. Our working hypothesis stemmed from the idea that there are other, more complicated methods that neural systems use to encode information, aside from simply counting a total number of potentials, or so-called "spikes", that occur in response to a single stimulus. Other sensory systems such as olfaction have been shown [45, 26] to use complicated spatiotemporal encoding schemes to transmit data that would initially appear to be lost through neural filtering. Since multiple neurons are recorded simultaneously with extracellular recording, the pattern in which each neuron fires can encode additional information that spike counting alone cannot reveal. This idea has been previously presented in

Theunissen[42], suggesting models for both visual and auditory systems.

3.1 Experimental Setup

In order to develop appropriate testing methodology, we made certain assumptions regarding the types of information which could be encoded by the cercal system and thus would be isolated during testing. We hypothesize that the ensemble neurophysiological activity in the ventral nerve cord is a function of the following parameters:

- stimulus **directionality**
- stimulus **frequency content**
- **habituation** - decreased sensitivity due to repeated exposure to similar stimuli
- **background noise** - stochastic resonance could improve sensitivity to low amplitude stimuli.

We paid careful attention to both the mechanical design of the testing apparatus as well as the features of the acoustic waveforms which would be used to isolate each feature for testing. Past studies by a number of research groups [22, 24] determined a simple method of producing simulated acoustic plane waves. They refer to this design as an “acoustic wind tunnel”. This setup consisted of a rigid tube cut in half and assembled around the completed cricket preparation, equipped with relatively small 6.5 inch mid-range drivers attached to each end. The speakers were wired such that they would operate 180° out of phase, in a so-called “push-pull” mode of operation. Theoretically this would be appropriate as the physical dimensions would only allow for modes which propagate axially down the tube.

3.2 Cricket Anatomy and Physiology

The nervous system consists of a dorsal cerebral ganglion (brain), a ganglionated nerve cord and a peripheral nervous system. A pair of circumesophageal connectives unites the cerebral ganglion and the subesophageal ganglion, the starting point of the ventral nerve cord. These structures are located in the head. The ganglionated ventral nerve cord exits the head and extends the length of the body along the ventral midline of the thoracic and abdominal hemocoel. The nerve cord includes three large segmental thoracic ganglia, which were linked to five smaller abdominal

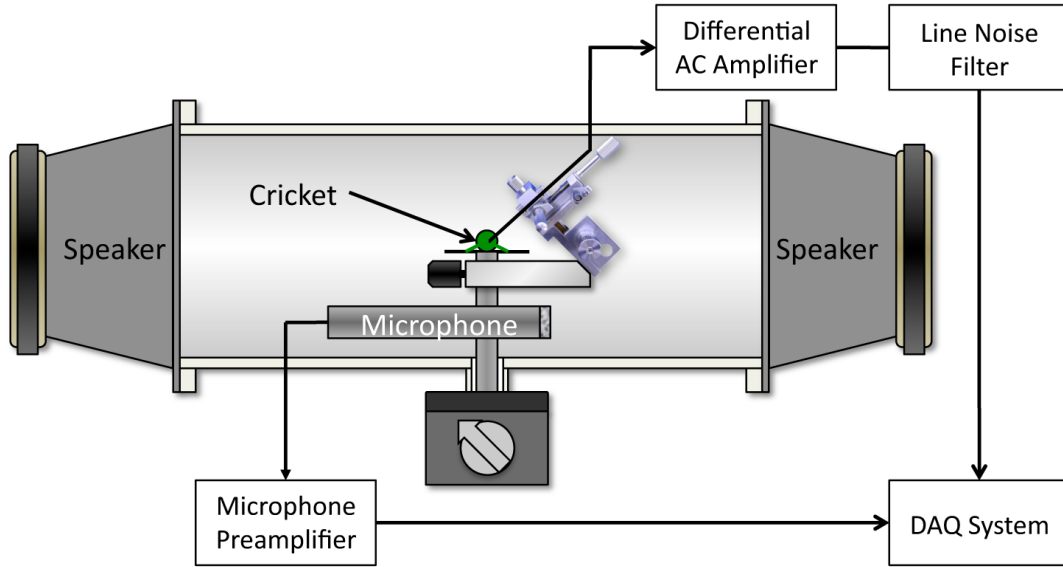


Figure 10: Acoustic response testing overview shows the electrical inputs and outputs of the experimental setup

ganglia through the longitudinal connectives. In the terminal abdominal ganglion (TAG), the fifth abdominal ganglion, the sensory neurons from the cerci synapse on the giant interneurons of the nerve cord. A rendering of this anatomy is presented in Figure 11.

The cerci are two conical abdominal appendages which are covered with about 1000 individual sensing hairs [28, 5]. There are three different types of hairs, which differ in both shape and function that will be described later. Each cercus is equipped with approximately 400 acoustically-sensitive filiform hair sensilla, which differ in length ($50\mu\text{m}$ – 1.5 mm) and diameter ($3\text{--}5\mu\text{m}$). The hairs insert into elliptically slotted, viscoelastic bases which constrain oscillation to one plane. Hairs are categorized by two types: lateral to medial oscillating hairs, and anterior to posterior oscillating hairs. However, these hairs are innervated in such a manner that the sensory neuron is only excited by movement in one direction. These four kinds of directionally sensitive hairs are not randomly distributed, but have a specific distribution pattern as shown in Figure 11d.

Another type of receptor on the cerci is the bulbous clavate hair [39] on the proximomedial aspect of the cerci responsible for the orientation within the gravity field. Each hair is innervated by a single sensory neuron that arborizes in the the Teminal Abdomial Ganglion (TAG). It is important to mention that the arrangement of directionally sensitive hairs on the cerci surface correlates

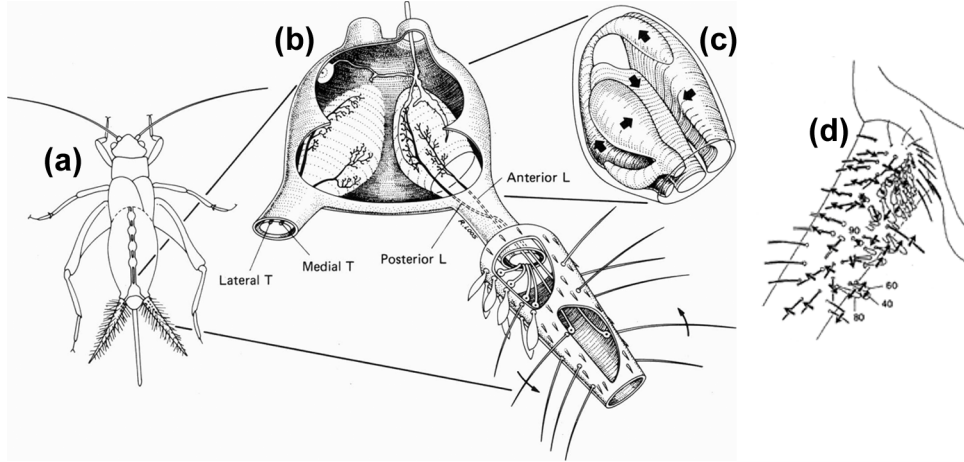


Figure 11: Anatomy of the cricket cercal system, reproduced from Bacon and Murphey, 1984 [2] **a.** ventral nerve cord **b.** Terminal Abdominal Ganglion (TAG) **c.** directionality mapping in the medial giant interneuron (MGI). The arrows represent regions in the TAG that are sensitive to excitation in the indicated direction. **d.** directional orientation of filiform and clavate hairs on a cercus, arrows indicate preferred motion of each hair

with the aborization of their afferents in the TAG. This means that there are four different, non-overlapping neuropile regions corresponding to different stimulus directions. The sensory neurons synapse on giant interneurons (medial giant interneuron MGI, lateral giant interneuron LGI) within the TAG. Hairs sensitive to different stimulus orientations are connected to different dendrites of the same interneuron. Hairs sensitive to the same stimulus direction but located on different areas of the cerci synapse to different interneurons [31]. This cross-referencing is what gives the cercal system the ability to gather so much information about the fluid field. Figure 11c displays arrows indicating the different directionally sensitive areas within the TAG.

3.3 *Multi-Unit vs. Single Unit Recording*

Depending on the dimension of the electrode tips, one has to distinguish between single-unit and multi-unit recording. Tips with a diameter up to $10\mu\text{m}$ were used for single-unit recording, which means that the diameter allows signal detection from just one neuron. Diameters over $10\mu\text{m}$ typically attach to more than one neuron, resulting in the term multi-unit recording. Common electrode materials are silver, gold, platinum or tungsten. Chloriding of silver electrodes improves the impedance of the electrode, which in turn increases recording sensitivity. Dual hook electrodes were used in this experiment constructed from two 0.008 in. diameter chlorided silver wires. Our

setup can be categorized as multi-unit recording.

3.4 Equipment

We developed two waveguide designs in this project, the initial setup was the design used by Jacobs and Kämper. When we tested for frequency response, a number of resonances were present in the spectrum between 5 Hz and 600 Hz, which is the region we planned to test in. We identified these resonant peaks as a Helmholtz mode and a cylindrical cavity mode using theory presented in § 3.4.1. The design was modified to eliminate an electrode access hole, and re-tested for frequency response. The resulting experimental setup is presented in Figure 12. We measured the frequency response for the updated design, which can be found in Figure 12d. The results show a reasonably flat useful region between 50 Hz and 550 Hz. We determined that this frequency band would be sufficient for testing.

An in depth account of the design and frequency response testing of the prototypes which lead to the final experimental setup design is located in Appendix A.4. For details of the acoustic equations used to develop and evaluate the waveguide designs as well as the stimulus signals used to excite the cercal system, see § 3.4.1; otherwise, skip to § 3.5 .

3.4.1 Acoustic Theory

In order to design an appropriate experimental setup to excite acoustic stimuli with well controlled parameters, the dimensions of the setup had to be carefully chosen to avoid resonances within the frequency range of interest. In order to design the dimensions of the tube described in Figure 10, predictions had to be made on the acoustic properties resulting from dimensional decisions, based on a cylindrical Helmholtz resonator. The anticipated stimulus frequency sensitivity of the cricket was within the range of 5Hz-600Hz, resulting in a design goal to incorporate flat response in as much of this range as possible.

3.4.1.1 Cylindrical Cavity Mode Calculation

Cylindrical modes were calculated such that the lowest resonances would be outside of the 5-600 Hz frequency range. Cylindrical cavities contain modes that propagate in both the longitudinal and radial directions, each of which must be calculated individually using theory developed in Kinsler

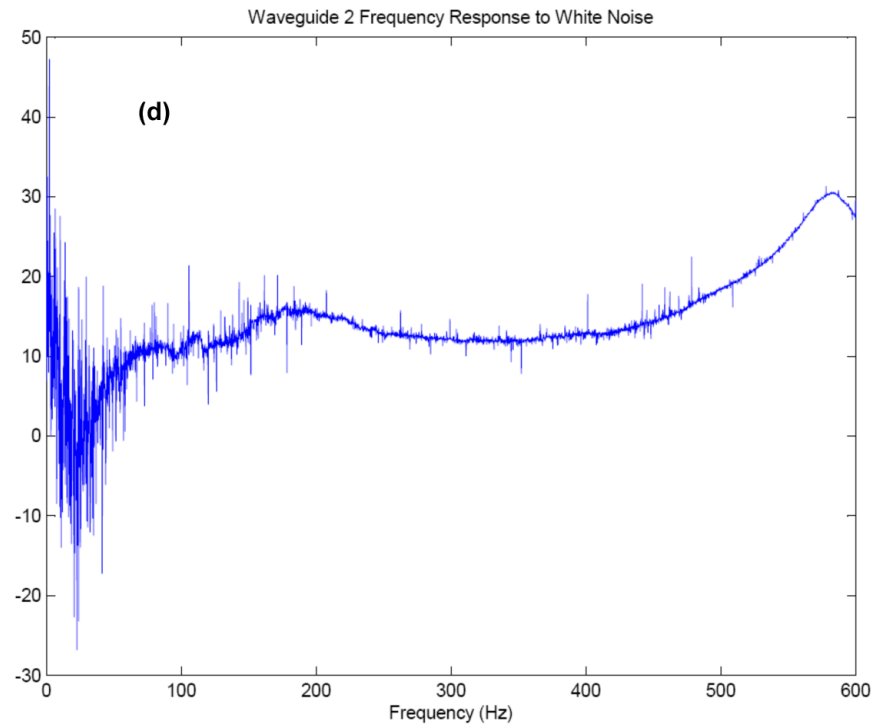
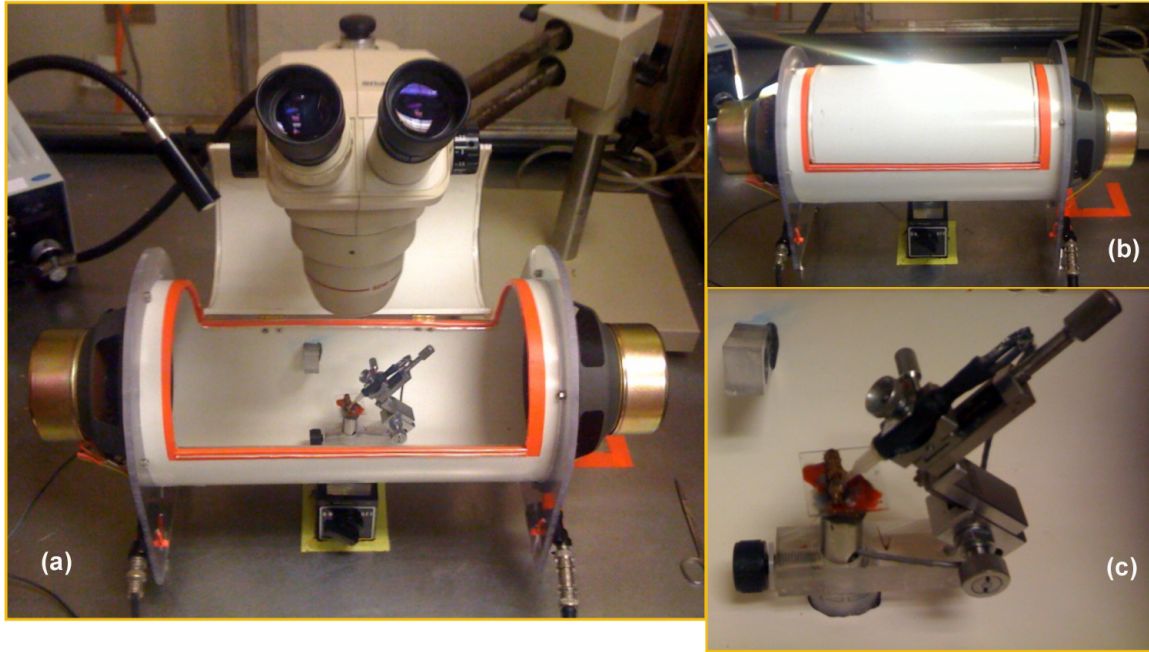


Figure 12: Design of testing apparatus 2. **a.** Fabricated waveguide. **b.** Sealed hatch access **c.** Internal micromanipulator mount. **d.** Frequency response spectrum of test apparatus 2.

[25] and Pearce [32].

Longitudinal modes in a cylindrical cavity are characterized by the form of Equation (1).

$$p(x) = A \sin \frac{n\pi x}{L} \quad (1)$$

where $p(x)$ is the acoustic pressure distribution along the length of the tube, A is the modal amplitude, n is the longitudinal mode number, and L is the overall length of the tube.

Radial modes are more cumbersome to calculate and are determined using Equation (2). The calculations assume rigid walls at all boundaries. Radial modes are classified using indices (q, m) , where q corresponds to radially nested shell modes, and m represents modes that split the circular cross section into semicircles or quadrants depending on the order. These modes are better described in Eriksson,[12].

$$\hat{p}(\vec{x}, t) = K_{q,m} e^{\pm i k_x x} J_m \left(\frac{\eta_{q,m} \zeta}{r} \right) \cos(m\phi) e^{-i\omega t} \quad (2)$$

where R is the radius of the cylinder. $\eta_{q,m}$ is the reference for each individual transverse mode and represents a number corresponding to the roots of the Bessel Function. $\eta_{q,m}$ are tabulated in Eriksson,[12]. From Equations (1) and (2), the resonant frequencies for each mode (n, q, m) can be calculated as shown in Equation (3).

$$f_{(n,q,m)} = \frac{c}{2\pi} \sqrt{\frac{\pi^2}{L^2} + \frac{\eta_{q,m}^2}{R^2}} \quad (3)$$

The first 3 modes (1,0,0), (0,1,0), and (0,0,1) were calculated and it was found that the original design with a 16 inch tube length created a (1,0,0) mode within range, so we adjusted it to 12 inches.

3.4.1.2 Helmholtz Resonance

Since the design developed by previous reserachers included a drilled hole for electrode access, the cylindrical cavity could be modeled as a helmholtz resonator. The fundamental resonance of this configuration is calculated using Equation (4).

$$f = \frac{2\pi}{c} \sqrt{\frac{S}{VL}} \quad (4)$$

where c is the speed of sound in air, S is the cross sectional area of the hole, V is the volume of the cavity, and L is the corrected neck length of the hole configuration. In this case the neck length was corrected for two end conditions of infinite baffles, one for the inside of the tube, the other for the outside of the tube. The total correction for L is $1.7r$, where r is the radius of the hole in the tube. The Helmholtz mode in the original configuration was found to be around 170 Hz. In order to eliminate this mode, the hole had to be eliminated, requiring redesign of the setup to incorporate the electrode mount within the tube.

3.4.1.3 Harmonic Signals

In order to determine the frequency and direction response characteristics of the cercal system, we designed appropriate stimulus signals to isolate each parameter. While the direction of the stimulus signal can be easily adjusted by rotating the waveguide, isolating frequency is difficult. The transient effects caused by the starting and stopping of a signal give rise to broad frequency content of the stimulus signal. In order to isolate a single, discrete frequency, an extremely long ramping up of the signal is required. Since the cercal system is subject to habituation, or desensitization to constant or repeated stimuli, the system would stop firing action potentials long before the acoustic stimulus ramped up to full strength.

In order to realistically apply discrete harmonic acoustic signals, Gaussian windowing was used to envelope the desired monotonic signal. A Gaussian window allows for a smooth rise and fall of the signal as well as giving absolute control over the frequency content of the stimulus. The main signal of interest would be a pure sinusoid, given by Equation (5).

$$p(t) = A \sin(2\pi f_c t - \phi) \quad (5)$$

In Equation (5), A is the amplitude of the excitation, f is the center frequency of the signal, and ϕ is the desired phase shift. Since this signal is only a pure tone if it exists forever, there is always a frequency adding effect associated with starting and stopping the signal.

3.4.1.4 Gaussian Windowing

In order to minimize the additional frequency content encountered, the Gaussian window described by Equation (6) is applied.

$$g(t) = \frac{1}{\sqrt{2\pi} \cdot \sigma} e^{\frac{-(t-T_S)^2}{2\sigma^2}} \quad (6)$$

In Equation (6), σ represents the standard deviation of the Gaussian curve in the time domain, and T_S is the time shift applied to the window. We apply $p(t) \cdot g(t)$, resulting in a Gaussian modulated sine wave, with a ramp time which we can adjust by varying the standard deviation, σ . The frequency spectrum of this wave also takes the form of a Gaussian bell curve centered on f_c . The bandwidth of the frequency content has an inverse relationship to the length of the time domain signal, ie. if the time signal is a short pulse, the frequency spectrum will have a large bandwidth.

In order to isolate the ramping shape, termed the “attack”, as a feature of interest, only the first half of the gaussian bell curve is applied to the pure tone. Once the maximum of the Gaussian is reached, the amplitude is held constant for the remainder of the signal. This resulting half-Gaussian shape (shown in Figure 14) is used for all subsequent testing.

3.5 Preparation Method for Extracellular Recording

Before dissecting the cricket, the specimen was chilled on ice for approximately 10 minutes to induce anesthesia. The wings were then removed and the cricket was mounted dorsally on a glass-surfaced magnetic base using a rosin-based sealing wax. Legs, antennae and the ovipositor (in case of a female) were removed to prevent measurement error due to electrode shifting resulting from random motion of the extremities. In the abdomen, the ventral nerve cord is typically located directly under the integument; as such, all transverse incisions have to be accomplished very carefully. Optimal recordings from the cercal system were expected between the terminal and the fourth abdominal ganglion. For this reason the 5th and the 6th sternite were removed by cutting laterally along the segments from posterior to anterior. The following transverse cut between the 4th and the 5th sternite had to be done with great care not to cut the ventral nerve cord. In most cases, the nerve cord is attached to the epidermis. To prevent the stretching of the cord by folding back the dissected part of the integument, it was necessary to separate the cord carefully from the epidermis using a pulled glass pipette, while simultaneously lifting the integument upwards with forceps. Once the 5th and 6th sternites were lifted vertically, a final cut between the 6th and the 7th sternite detached



Figure 13: Dorsally mounted prepared cricket with dual hook extracellular electrodes placed under the ventral nerve cord. The wire wrapped around the cricket serves as a grounding reference.

them from the rest. The nerve cord was occasionally covered by a layer of fat, which had to be removed carefully with a glass pipette or forceps. The nerve cord is semitransparent and difficult to detect. A few drops of saline served as a lens and increased the chance of locating it in addition to preventing the cricket from desiccating. See Appendix A for saline formulation. The dual hook recording electrodes were placed under the cord using a mechanical micromanipulator and slightly lifted from the abdomen. In order to increase the signal to noise ratio, a KimWipe was used to absorb the saline between the cord and the abdomen. A mixture of Vaseline and mineral oil was applied over the nerve cord and abdomen using a syringe, in order to reduce motion of the nerve cord and to decrease the desiccation rate. Figure 13 shows a cricket prepared for extracellular recording.

3.6 Data Acquisition and Experimental Methods

Data acquisition was accomplished using a National Instruments NI 9234 connected to a USB port via NI's CompacDAQ system. The board is designed for sound and vibration measurement and includes filtering circuits to perform anti-aliasing prior to data acquisition. The maximum sampling

Table 3: Amplifier Settings

Equipment	Control	SetPoint
X-Cell3+ Differential AC Amplifier	Gain	10,000x
	Low Frequency Cutoff	100Hz
	High Frequency Cutoff	10,000Hz
Sony STR-DH100	Volume	+30
	Bass	+10
	Treble	-10
	Mode	External

rate of 51.2 kHz was used for the majority of the testing reported herein.

Each prepared cricket was tested for a total of two trials. Collection of larger data sets would require a far less invasive method of electrophysiology such that the preparation could last longer, as each data set is quite time consuming. Once the cricket was prepared, dissected, and probed with extracellular recording dual hook electrodes, the waveguide was sealed and oriented at 90° with respect to the animal’s ventral centerline. The amplifier settings used for extracellular recording are presented in Table 3.

The first experiment was designed to determine the effects of envelope shape and stimulus center frequency on total spike response. In order to calibrate the spike counting routine, the first recording was taken without an acoustic stimulus. The purpose of this trial was to gauge the baseline activity within the nerve cord. The highest amplitude activity at this resting state was recorded and used to set the amplitude threshold for the spike counting VI. A Gaussian standard deviation was selected and the sound files, with center frequencies ranging from 50 to 600 Hz were played in ascending order in 10 Hz increments while recording the cricket’s cercal system response. This was repeated for each standard deviation value tested, including envelope standard deviations (σ) of 0.005, 0.05, 0.15, and 0.25. In all cases the envelope was delayed for 5 seconds, with each stimulus lasting a total of 10 seconds. This time delay allowed the cricket’s sensory cells to regenerate before the next trial.

The effect of habituation was measured next using white noise enveloped with half-gaussian functions. White noise was used to eliminate any effects caused by varying the center frequency. The same four standard deviations used in the frequency measurements were tested. Each signal

was played 20 times back to back while recording extracellular response. Spikes were isolated and counted at the end of each exposure.

In order to determine the directional sensitivity of the crickets, the waveguide was rotated in 30° increments and measurements were repeated until 180° information was obtained. Only 180° of information was necessary since the directionality is identical from either side of the cricket due to the presence of a driver at each end of the waveguide. The total number of spikes in response to each stimulus was recorded.

All testing was repeated for five (5) specimens, creating a statistical sample population of $n = 5$. Future work should involve repeating these measurements for additional specimens in order to create a larger sample size.

3.7 Results

For each of the trials described, 10 seconds worth of extracellular data was recorded. Within LabVIEW, the data was analyzed in order to determine the locations of individual spikes. In order to minimize the hard drive space and processing power required, the spike temporal locations only were recorded. For each envelope shape, the fully sampled 50 Hz trial was recorded to ensure that spikes were individually separable and that super-threshold responses were not caused by separate spikes aligning temporally, creating an additive effect. An example of the half-gaussian stimulus signals used, the raw data recorded from the cricket, and the data after processing to isolate spikes is presented in Figure 14.

As shown in Figure 14b., the cercal response occurs mainly during the ramping period of the stimulus signal, and is characterized by spikes with much larger amplitude than the spikes which occur naturally before the stimulus is presented. The variation in spike amplitude is expected as a result of the multi-unit extracellular recording picking up signals from multiple neurons at once. Previous studies have shown that the action potentials produced by the MGI and LGI tend to have increased spiking amplitude in comparison to surrounding neurons. We verified that the amplitude variation was indeed individual spikes, and not an additive effect of multiple neurons firing simultaneously by isolating individual spikes and verifying the expected shape presented in Figure A.1.

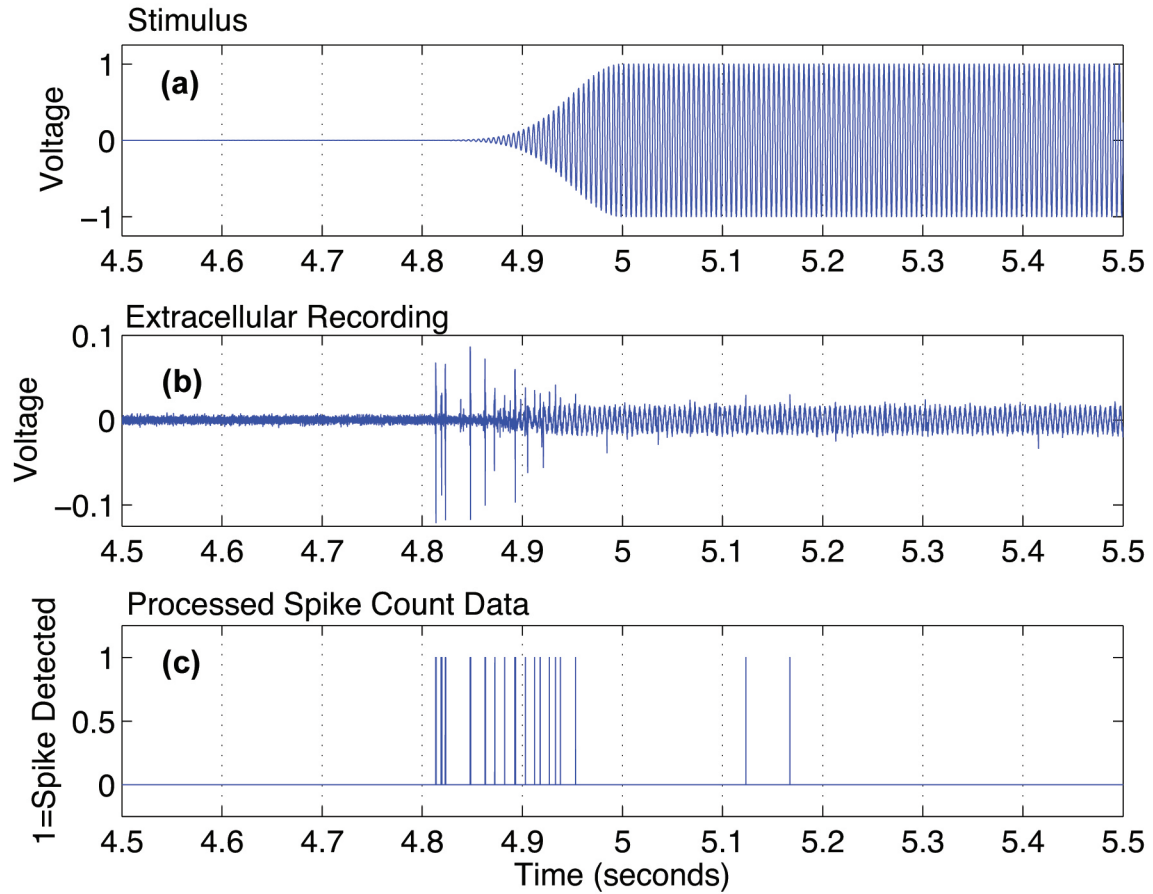


Figure 14: Example showing the signals pertinent to testing **a.** Stimulus: Half-Gaussian modulated acoustic signal with 60 Hz center frequency and $\sigma = 0.05$ **b.** Response: Raw extracellular cricket response data in response to a taken from the ventral nerve cord **c.** Processed Response: Data from b post-LabVIEW processing to isolate individual spikes.

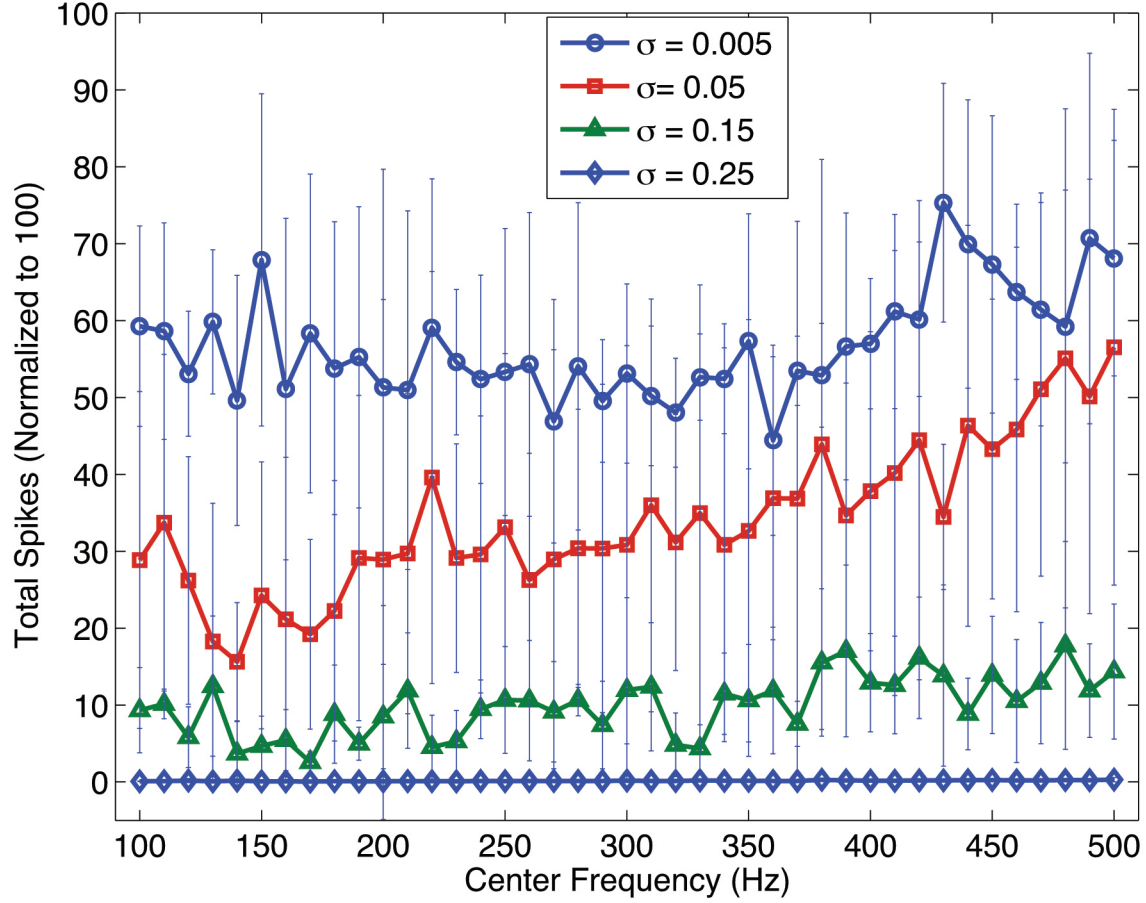


Figure 15: Total spike response as a function of center frequency for four various Gaussian standard deviations. Error bars indicate the statistical standard deviation for each measurement reported based on the population of 5 normalized data sets averaged.

3.7.1 Response to Varied Center Frequency and Ramp Shape

The total spike count data from five(5) crickets was combined by normalizing each animal's data by its largest spike total. The normalized data was then multiplied by 100 to represent each spike response as a percent of it's maximum response. The statistical mean and standard deviation of the five data sets was calculated for each frequency and data sets were separated by Gaussian standard deviation, σ . Although data was recorded using center frequencies from 50-600 Hz, data is only reported from 100-500 Hz since this is the operating range of the waveguide that we feel most comfortable reporting data from. Figure 15 shows the data for each envelope used, along with error bars indicating the statistical standard deviation for each frequency.

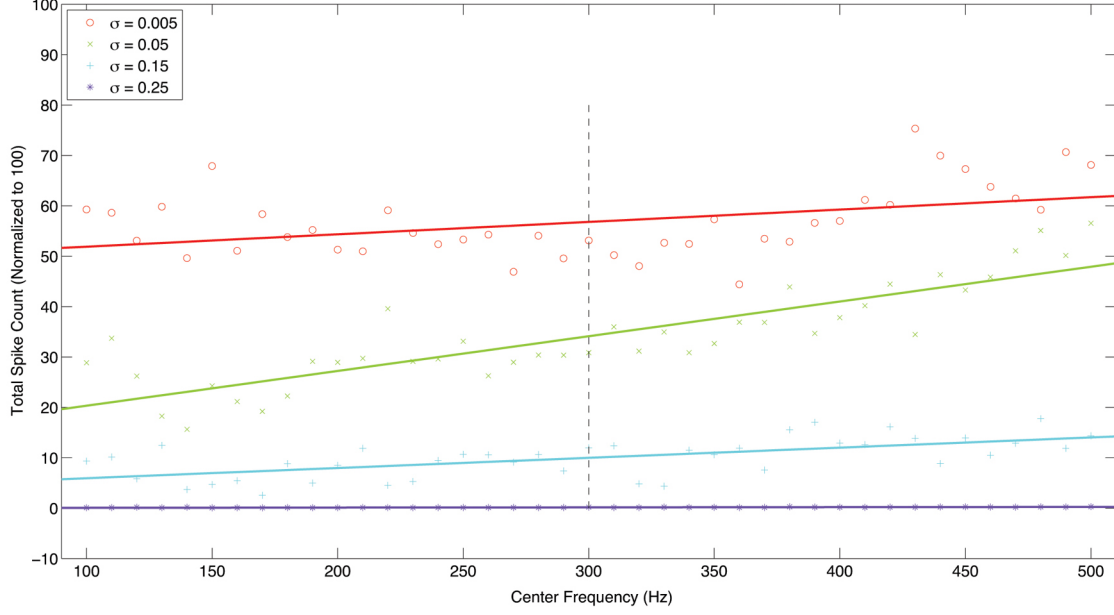


Figure 16: Analysis of Covariance (ANOCOVA) for the averaged normalized data sets from a sample population of 5 crickets. Analysis uses σ as the regression variable and tests for covariance with center frequency, f_c .

The data in Figure 15 shows almost horizontal trends for each value of σ and an overall increase in the mean spike count with decreasing σ . If these results are accurate, we can draw the conclusion that total spike count is not a function of center frequency but does on the value of σ . In order to determine the accuracy of this statement, statistical analysis was performed on the data populations using analysis of covariance (ANOCOVA) methodology to determine if the mean of each curve, determined by the y-intercept, is really different from other curves and whether or not the value covaries with both σ and f_c , determined by the slope of each curve. This analysis was performed using the Statistical Analysis Toolbox in Matlab. Figure 16 shows the resulting plot from the ANOCOVA analysis. The resulting coefficients determined through ANOCOVA analysis are presented in Table 4.

The result of ANOCOVA analysis is that crickets are not sensitive to variations in center frequency, but rather to the transient amplitude effects caused by enveloping of the signal. This conclusion has not been previously published.

Table 4: ANOCOVA Coefficients

Term	Estimate	Standard Error	T	Prob.> T
<i>Intercept</i>	16.703	0.9259	18.04	0
$\sigma = 0.005$	32.729	1.60371	20.41	0
$\sigma = 0.05$	-3.271	1.60371	-2.04	0.0431
$\sigma = 0.15$	-12.786	1.60371	-7.97	0
$\sigma = 0.25$	-16.672	1.60371	-10.4	0
<i>Slope</i>	0.029	0.00287	9.94	0
$\sigma = 0.005$	-0.004	0.00497	-0.8	0.4253
$\sigma = 0.05$	0.04	0.00497	8.13	0
$\sigma = 0.15$	-0.008	0.00497	-1.67	0.0966
$\sigma = 0.25$	-0.028	0.00497	-5.66	0

Table 5: ANOVA Coefficients

Source	d.f.	Sum Square	Mean Square	F	Prob.> T
σ	3	79412.2	26470.7	1398.61	0
f_c	1	1869.3	1869.3	98.77	0
$\sigma \cdot f_c$	3	1440.3	480.1	25.37	0
Error	156	2952.5	18.9	-	-

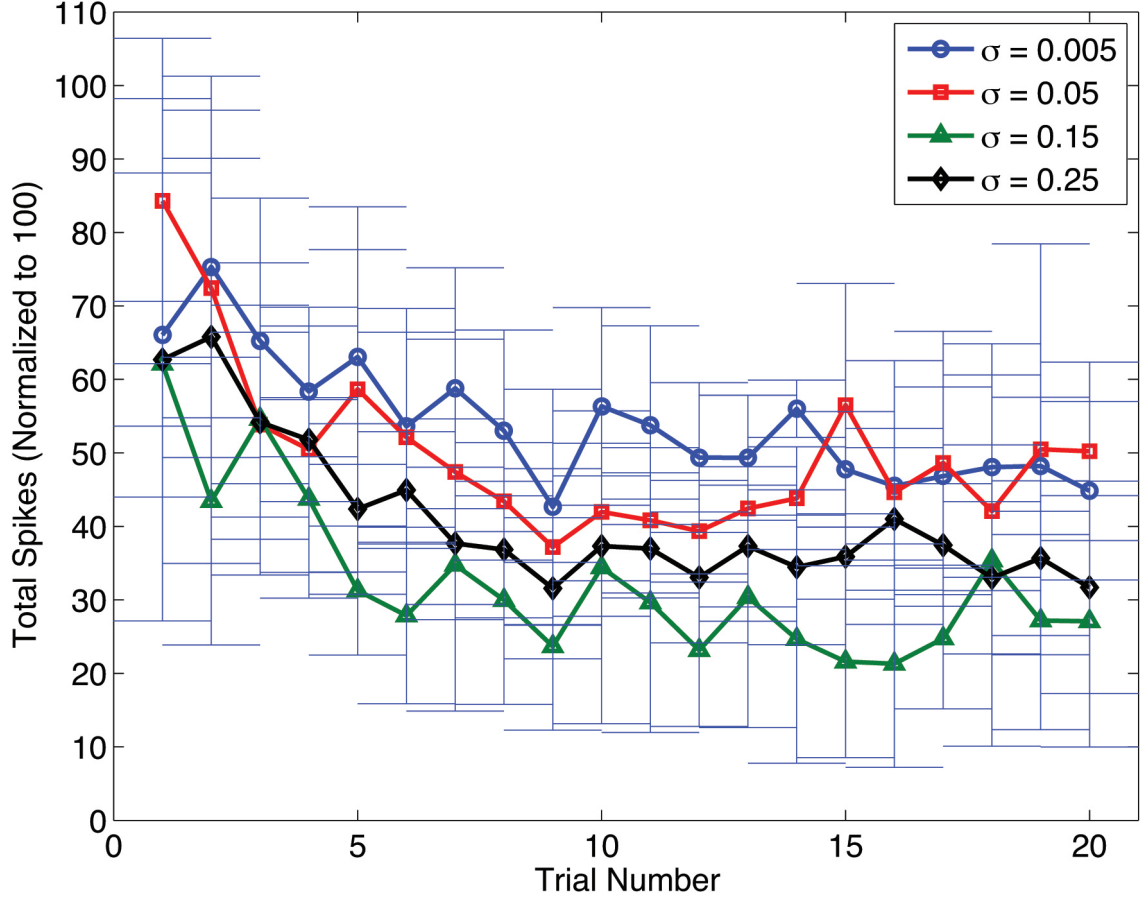


Figure 17: Habituation to repeated stimuli. Total spike response to Gaussian enveloped white noise as a function of trial number. Plot shows a clear decline after the initial exposures, leveling out to a habituated response level. Error bars represent the statistical standard deviation for the sample population at each data point.

3.7.2 Habituation Effect on Response

In order to quantify the effect of habituation, crickets were repeatedly exposed to a Gaussian-bounded white noise signal. The stimulus was applied 20 times in a row for each σ and the total number of spikes were recorded for each trial and plotted as a function of trial number. The resulting plots, shown in Figure 17, show the habituation rate as a function of envelope shape. As with the previous data analysis, the data for 5 individuals was normalized, then averaged with the rest of the data.

Based on the results presented in Figure 17 an exponential relationship can be derived between total spike count and number of repeated exposures. This relationship takes the form shown in

Equation (7).

$$H(n) = Ae^{-bn} + C \quad (7)$$

Where A , b , and C are generic constants, and n is the number of exposures to the same stimulus. The large error bars associated with each data point overlap with other data points for different σ 's, which indicates that habituation rate is not a function of the envelope shape. This means that the cricket would have the same percent habituation by trial regardless of the stimulus that is used.

3.7.3 Cercal System Directional Sensitivity

Although it has been long known that source direction can be extracted from the cercal system's ensemble activity, we verified this experimentally and also tested whether or not envelope shape has an effect on directional sensitivity. It has been commonly accepted in past literature that the directional response to sound takes the shape of a half-cosine with the maximum response when the orientation of the stimulus is parallel to the body of the animal. Our results show minimum sensitivity perpendicular to the animal's midline. Data for five crickets was normalized according to σ by the largest response in each animal, then averaged across specimen. The normalized directional sensitivity plots are shown in Figure 18.

The plot of directional sensitivity shows that the shape of the envelope has no effect on the directional response of the cricket, it simply amplified the total spike count as a function of ramp sharpness. This means that the directionality can be decoupled from the frequency content of the signal. By networking multiple crickets, at least two, the directionality and envelope information can be separated and therefore quantified.

3.7.4 Response to Background Noise

Many research efforts have attempted to quantify the neurological response to different bandwidths of white noise. One of the hypotheses in this project was that eventually the cercal system would completely habituate to any background noise after a sufficient amount of time, which turned out to be incorrect in practice. If confirmed it was planned to use this white noise to mask the sinusoidal stimulus signals in order to determine the minimum signal to noise ratio that could still be detected by the cerci. White noise was filtered over two different bandwidths, 20-70 Hz, and 50-550Hz. The cricket was continuously subjected to this sound over the course of 120 seconds while neural response

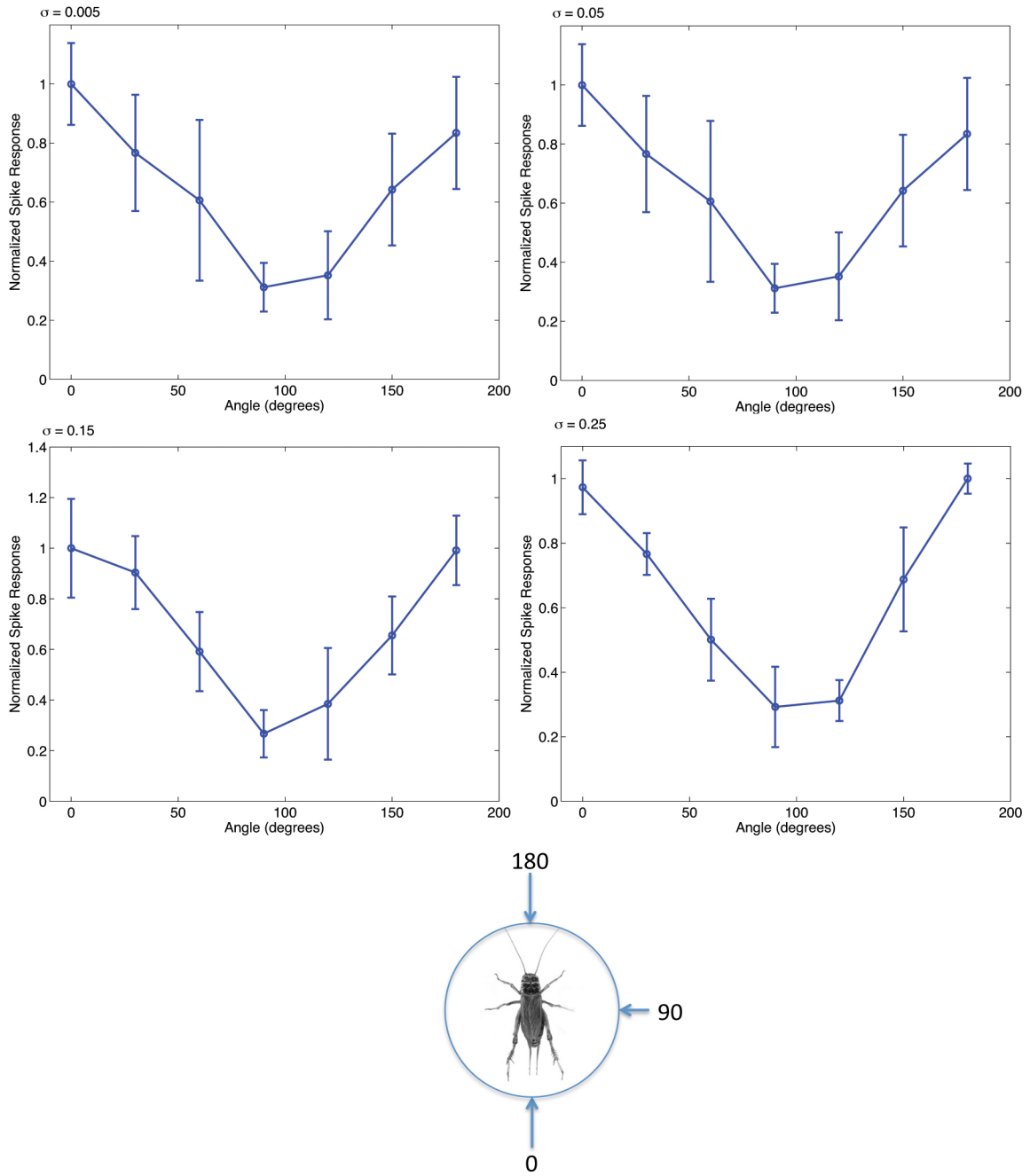


Figure 18: Normalized directional sensitivity response to stimulus reported by Gaussian envelope parameter σ . The overall shape does not depend on the value of σ

data was recorded. As shown in Figure A.5, the cricket never fully habituated to the white noise stimulus. The reason for this inconsistency could be due to some non-linear artifacts of the drivers when driven with white noise, resulting in transient effects which the cricket cerci can sense. This result led to the abandonment of this measurement task, and thus we were unavailable to examine the effect of background noise on cercal sensitivity.

3.8 Discussion

We have determined that crickets are not sensitive to variations in the center frequency of sounds, confirming the hypothesis posed by previous researchers. Instead, **crickets are sensitive to transient effects of amplitude changes caused by enveloping functions**. Larger sample populations could be used in the future to minimize the error bars shown in Figure 15. This result is important because it shows that the cercal system is incapable of detecting continuous signals. Additional spatiotemporal analysis of the signals could be the process needed to uncover the information about center frequency content, which is not obtainable through spike counting alone. While current technology makes this task feasible, the lack of project funding for costly software and computing power were unavailable to the current study.

The results of this portion of the study indicate that the process of counting the total number of threshold spikes for a given stimulus is sufficient to estimate both the direction and the temporal scale of the enveloping function used to stimulate the cricket. The center frequency of the signal; however, cannot be determined using this method as evidenced by the identical response measured when using Gaussian modulated sine waves and Gaussian modulated white noise stimuli. Additionally, the history of sounds the cricket has been exposed to must be known in order to estimate the effects of habituation to each response.

CHAPTER IV

IMPLANT DEVELOPMENT

In order to use the cricket as a novel sensor, we developed a method of permanent implantation of an extracellular recording electrode. Tobias Horstmann, an 2009 summer intern, was instrumental in this development process, providing extensive knowledge in neurobiology, electrophysiology, and biomimetics. The final result was an effective dual hook electrode design and a manual installation procedure detailed herein. We implanted a total of 4 crickets, and compared successful measurements from one cricket with measurements taken using the procedure described in Chapter 3. Our best application was able to survive a total of 6 days with an implanted electrode.

4.1 Implant Design

The first design of the implant electrode was constructed with tungsten wires isolated in a glass tube. The main idea was not to attach the wires to the nerve cord, but to determine the healing abilities of the harmed integument and the survival period after such an implantation. Moreover, the influence on locomotion and ingestion of food was examined. The results were not satisfying, and therefore the glass tube was left out of the second design. The wires were coated by a thin layer of red rosin wax. The crickets were able to recover quickly from this implantation but only survived for the next 48 hours. The wax coat; however, did not always prevent the two tungsten wires from touching, requiring other coating methods.

It was determined that Teflon[®] coated silver wires would be used as implantation electrodes. This was decided based on testing with a number of different electrode materials to determine which allows the greatest signal to noise ratio. The PTFE-coated silver wires (A-M Systems, Inc., WA, USA) had a diameter of .1778mm, and a Teflon[®] layer thickness of .0254mm. Two pieces of wire were cut to the same length of approximately 25mm. Under a dissection microscope the Teflon[®] coating of each end was carefully removed using either a hot needle or a scalpel. 2mm of Teflon were removed from the end to be attached to the nerve cord. About 5mm of the Teflon[®] coating was removed from the end that would protrude the cricket. Next, the two wires were placed parallel on



Figure 19: Permanently implantable electrode design consists of two Teflon coated silver electrodes bonded with epoxy. The hooked end is implanted around the ventral nerve cord and the opposing end protrudes from the dorsal integument of the cricket.

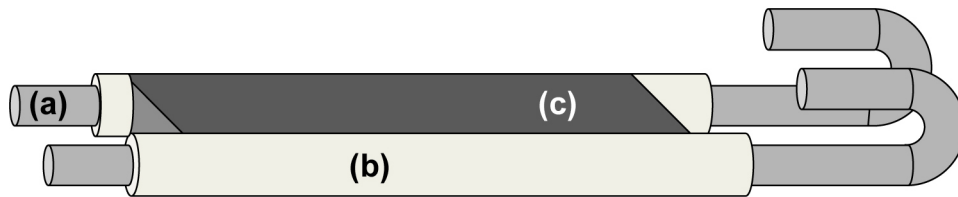


Figure 20: Permanently implantable electrode schematic. Overall length of electrode is 25 mm. Wire diameter is .1778 mm. **a.**Silver wire **b.** Teflon coating **c.**Epoxy bonding

two small dental wax balls with a small gap in between, the width of two wire diameters. The two wires were then bonded together (Kwik[®], J-B Weld Company, USA) to increase the rigidity of the implant electrode. After the epoxy hardened, the short end tips were bent into a hook-shape using forceps, which assured the attachment to the nerve cord, whereas the bend shapes differ depending on the implantation method. Figure 19 shows the completed electrode fabrication.

4.2 *Surgical Procedure*

The main difference between the surgical procedure for permanent electrode implantation and the dissection for extracellular recording is that in the case of the implantation, all cuts had to be small enough to facilitate healing. Tissue could not be removed, nor could organs be damaged. The best way to access the nerve cord was from the ventral side. Two cuts on each side of the 6th sternite had to be done and one further cut between the 6th and the 5th. The most appropriate tools for making this incision was stainless dissection scissors. These three cuts allowed the peeling back of the 6th sternite. A few drops of saline held the sternite back, so that the nerve cord became visible

without removing any integumental tissue. To implant the wires into the cricket we attempted two different surgical procedures. One solution required the wires to come out of the cricket ventrally (ventral implantation), the other one implied the wires to protrude dorsally (dorsal implantation). For the latter solution, another longitudinal cut through the 6th tergite (dorsal counterpart of the sternite) had to be made, in order for the wires to protrude. It is important to note that the terms ventral implantation and dorsal implantation do not refer to where the wires were implanted but rather where the wires exit the cricket.

4.2.1 Anesthesiology

In order to perform the surgical implantation, an alternative anesthesia method other than chilling with ice was required to incapacitate the cricket over a longer period of time, since the animal had to be completely asleep in order to perform the delicate manipulations required. The following anesthetic substances were tested:

- Chloroform
- Isoflurane
- Difluoroethane gas
- CO₂ gas

Best results were achieved with Difluoroethane. A 15 minute treatment in a 1 liter glass flask anesthetized the crickets up to 20 minutes, providing enough time for the surgical procedure and the implantation of the silver wires. The practice of chilling on ice used for the dissection emerged as inappropriate for surgery. It provided sufficient time to mount the cricket on the glass-surfaced stand and to remove the extremities, leaving the cricket in a state in which it is unable to move; however, it doesn't provide enough time to carry out the entire implantation procedure including the surgery. Chloroform and CO₂ had similar effects to chilling on ice. CO₂ is an appropriate anesthesia method, as long as there is a constant CO₂ flow during the surgery and implantation. Isoflurane is an anesthetic normally used for large vertebrates, making it difficult to determine the appropriate dosage.

4.3 Ventral Implantation

In order to perform the ventral implantation the anaesthetised cricket was placed in a modified Eppendorf[®] tube, which was mounted on a stand. The cricket was fixed with two strips of dental wax to keep it in place during the implantation, as this procedure requires absolute motionlessness of the crickets body. The two silver wires were waxed on the end of a ca. 100 mm steel bar. A 150 mm steel wire was coiled around the bar behind the wax, connected to a DC power supply (HY3003, MASTECH[®]). The bar was placed in a micromanipulator with three moving axes. A 10x- to 20x magnification was used to attach the implant electrode to the nerve cord. Depending on the angle of the micro-manipulator, and thus the angle of the implant electrode, another longitudinal cut through the middle of the 6th sternite could be made, where the wires were expected to penetrate the integument. The folded back abdominal segment was then returned to its original position. The cuts tend to heal in approximately 24 hours. One drop of hot sealing wax was applied to the wires where they come through the cuticle to prevent the electrode from losing its connection to the nerve cord. Finally the power supply was switched on to 3V, allowing the inductor coil to melt the sealing wax, separating the electrodes from the steel bar.

4.4 Dorsal Implantation

For the dorsal implantation the cricket was placed in a modified Eppendorf[®] tube the same way as for the ventral with the slight difference that the tube had a small hole which aligns with the small incision in the 6th sternite described in section 4.2. The term “dorsal implantation” might be a bit misleading since the wires were implanted from the ventral side; however, they are supposed to come out of the dorsal side. Two methods of implantation were attempted manually and with a micromanipulator. A device was build for the micromanipulator that could be affixed and re-affixed to the electrode easily, whereas the electrode had to be inserted in a capillary glass tube. Implantation by hand was simply done with two forceps. For the dorsal implantation, only mature female crickets with full ovaries were chosen. That is because the wires have to be pierced dorsoventrally through the cricket without harming essential organs. Mature ovaries expand within the hemocoel and move organs like the intestines, as well as the colon out of the way, so that they remain intact during the implantation. Beginning with the straight end the electrode was pierced

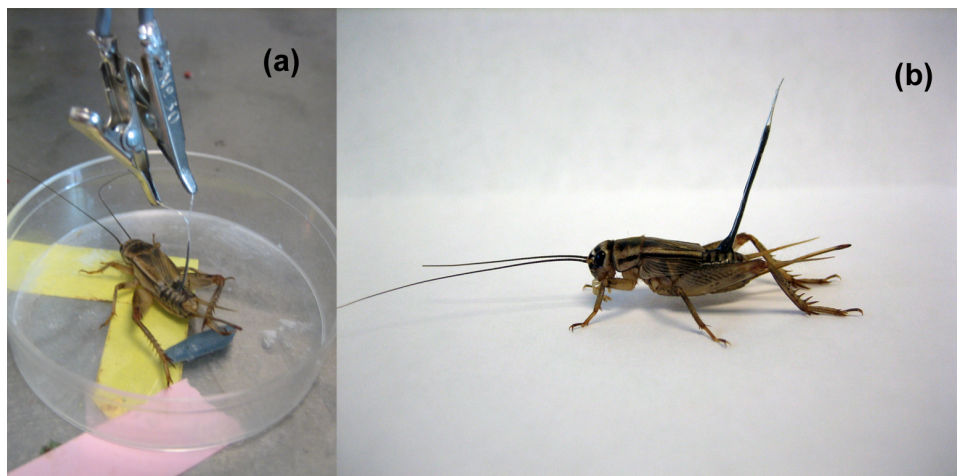


Figure 21: Robocricket **a.** Cricket with dorsally projecting implant electrode **b.** Free cricket connected to amplifier

through the ovaries either carefully by hand using forceps or with the micromanipulator. The next challenge was to get the end of the electrode through the small incision of the 6th tergite on the dorsal side. After that, either the forceps or the micromanipulator were reattached to the straight end of the electrode coming out of the dorsal side to bring the hook-end of the electrode in contact with the nerve cord. Finally one drop of either sealing wax or epoxy was used to seal the incision on the tergite where the electrode exits. Figure 21 presents the final design and implementation of a permanently dorsally implanted cricket.

4.5 *Implant Results*

The best results were achieved with a dorsal implantation installed by hand. Ventral implantation revealed the following problems: The equipment (amplifier, battery module, miniature radio transmitter) required for the cricket cyborg is intended to sit in a compact unit on the crickets back. For the amplification of the signals recorded from the implant electrodes, the shortest distance between the electrodes tip and the amplifier yields the minimum amount of noise. The shortest path is obviously straight through the crickets dorsal surface, instead of wrapping the electrode around the cricket from the ventral side to the amplifier. Moreover, after a ventral implantation the cricket must remain fixed in the Eppendorf tube for 24 hours, whereas after dorsal implantation the cricket can be placed in an isolated box immediately, providing liquids and solids to recover

from the surgery. In order to perform a dorsal implantation using a micromanipulator the implantation electrode must be placed in a glass capillary tube. This increases the diameter considerably, causing more damage to the inner organs during implantation. Moreover, the glass electrode is heavier and thus has influence on the crickets locomotion. Dorsal implantation by hand is quite a delicate operation requiring steady hands; however, it was possible to get clear measurements of action potentials from the electrodes implanted using this method (see Figure 22). Measurements were made approximately 4 days following the cricket's surgery, and recordings were possible for an additional two days following the initial measurements.

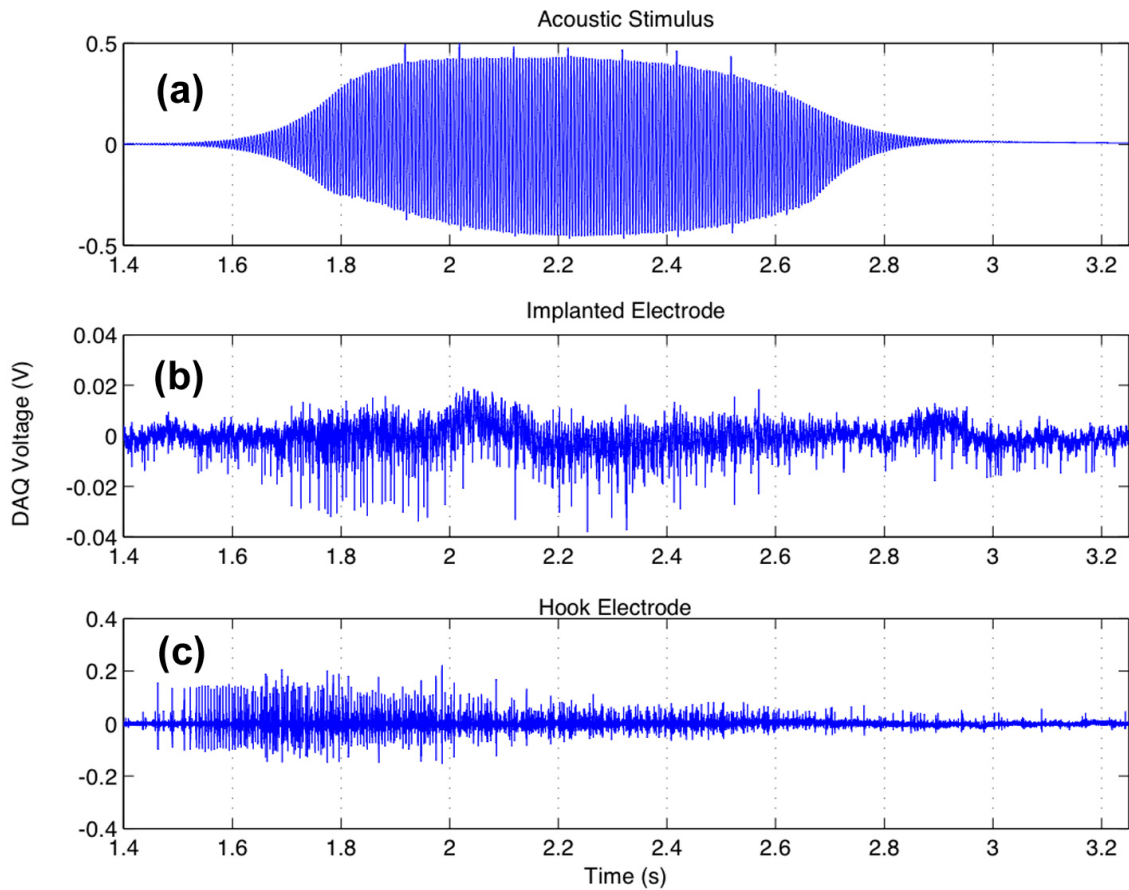


Figure 22: Comparison of signals obtained by robocricet to the signals obtained with standard extracellular recording **a.** Gaussian ($\sigma = .015$) Modulated 200 Hz sine wave **b.** Response measured from the implanted electrode **c.** Response measured from standard extracellular recording

4.6 *Discussion*

The comparison of the results measured from previous extracellular recording and the results obtained from the cybernetic cricket (Figure 22) reveal that latter one shows a lower spiking amplitude to the same acoustic stimulus (200Hz). Moreover, data acquisition from the implantation electrode were limited, such that no significant conclusion can be drawn from the spiking response. The results obtained are sufficient to demonstrate that it is possible to detect neural activity utilizing a permanently implanted electrode. The signal to noise ratio could be improved for the implanted electrode with the design of a better sealing mechanism around the electrode/nerve cord interface. The fact that the electrode tips are able to touch other adjacent organs and tissue masks some of the signals from the ventral nerve cord. The use of a higher amplification factor could also compensate for the lack of sensitivity of the implanted electrode.

CHAPTER V

CONCLUDING REMARKS

This project examined the use of crickets as a biosensor to detect and localize low frequency stimuli. The results of the previous sections indicate that the cricket is not suitable for use as a directional microphone as originally intended. Instead it is more suited for use as a vector sensor [9] that senses changes in the acoustic field. Although the cricket's neurological system is much more complicated than we originally anticipated, significant signal processing has allowed for the extraction of some useful information from the spike train generated by the cricket's Terminal Abdominal Ganglion.

Behavioral testing showed that the previous assumption that crickets exhibit negative phonotaxis is not correct. Exposure of the cricket to low frequency acoustic cues and standing substrate waves revealed an exception. If a path of minimum surface velocity exists, crickets will generally take this escape route. If the vibration node line is oriented in toward the sound source, the cricket will most often violate this negative phonotaxis relationship and move toward the sound.

Neurological testing revealed a few new insights and confirmed the directional sensitivity of the cercal system proposed by previous researchers. Using extracellular recording of the ventral nerve cord a relationship between spike trains and the acoustic stimuli the elicited them was developed. We determined that neurological response is a function of sound direction, envelope shape, and pre-existing behavioral conditions such as habituation to repeated stimuli. An inverse relationship between the number of spikes generated and the temporal standard deviation of the acoustic stimulus was found. This indicates that the cricket's escape response is most sensitive to stimuli that occur very abruptly, which can yield the relationship that the broader the frequency of a stimulus, the more response is evoked.

Finally, a design and surgical methodology were developed for a permanently implanted extracellular electrode which could allow the cricket biosensor to operate autonomously and remotely from the processing station. Successful implantation allowed for recordings to be made and compared with standard extracellular methodologies, proving the viability of the implant. Additionally, the

implanted cricket was able to survive for approximately seven days, demonstrating that long-term survival of an implanted cricket is possible if a more precise method is developed.

5.1 Future Work

The main issue not resolved in this research was the real-time resolution of cricket data into acoustic information. In order to fully describe the acoustic field, the spike trains measured would need to be decoded using a spatiotemporal pattern analysis tool. This type of analysis requires equipment and funding outside the scope of this project.

In order to develop a fully autonomous system, the extracellular setup would need to be completely miniaturized. A miniaturized differential AC amplifier and wireless transmission radio would have to be designed. In order to power the sensor, an energy harvesting device and battery would also require miniaturization. The LIMS group has spent significant resources developing implantable electrodes in moths, which are installed during the developmental instars and become an intrinsic part of the insect [34, 35, 38, 37, 36]. This portion of their research is directly valuable to the cricket biosensor research. Additionally, LIMS has begun development of energy harvesting methods from moth locomotion in order to power the onboard electronics, developing a completely self-sustainable system, and reducing the requirement for bulky battery packs.

Networking of multiple cricket biosensors could be used to develop improved angular resolution capability of the system. Further signal processing methodology could be borrowed from acoustic array processing standards, and each cricket could be fitted with a GPS unit to relay its location to a central processing station.

APPENDIX A

WAVEGUIDE TESTING AND EXTRACELLULAR RECORDING METHODOLOGY

A.1 Saline Solution

In order to lubricate the cricket during the dissection and recording process, while maintaining its delicate internal chemistry, a saline formula had to be derived. The saline was composed of the three different solutions as suggested by Dr. Richard Vogt of the University of South Carolina:

Table A.1: Saline Formulation

Component	Compound	Quantity
Solution A - 100 mL	NaCl	9.06g
	KCl	0.52g
	MgCl ₂ * 6 H ₂ O	0.81g
Solution B - 100 mL	NaCO ₃	0.21g
Solution C - 100 mL	CaCl ₂ * 2 H ₂ O	1.174g

To make 100mL of cricket saline 10mL of Solution A and 10 mL of Solution B were added to 70mL of distilled H₂O. Subsequently, the pH-value was monitored with a pH-meter. Either 10% HCL or 10% NaOH was added to adjust the pH to 7. When the solution was neutral, 10mL of Solution C was added slowly, while stirring.

A.2 Extracellular Recording

Extracellular recording is one of two methods typically used to record neural activity. Neurons communicate by local changes of the transmembranal voltage-differences that propagate along the axon. These local voltage changes are called action potentials and occur through ion flow over the membrane, where sodium and potassium cations and organic anions play an important role. A neuron, or rather an axon, at rest has a voltage difference of approximately -70mV in the inside with respect to the outside. This state is called resting membrane potential and based of the ratio of differently charged ions across the membrane. The maintenance of this ratio is based on an energy

consuming process; however, this ratio can change through an input of ions (mostly sodium cations) from a variety of sources, such as chemical synapse, sensory neurons or changes in the environmental ion distribution. If the variations of the ion-ratio, which determines the resting potential, reach a specific threshold, voltage-sensitive ion channels (Na^+ and K^+ channel) change their conformation which causes Na^+ flux into the cell and K^+ flux out of the cell. This phenomenon is called action potential, as mentioned above. These fluxes of sodium and potassium ions occur temporally delayed, which results in a temporary (approximately 1ms) increment of positive charge in the inside with respect to the outside (approximately +40 to +55mV) . This phase is called depolarization; the following return to the initial state is called repolarization. Action potentials always occur at one point of the axon and propagate in one direction by depolarizing environmental membrane areas, which opens further voltage-sensitive ion channels. Extracellular recording detects these local voltage changes and thus provides information about the number and intensity of action potentials in form of so called spikes, which can be amplified and recorded through data acquisition. The greatest advantage of extracellular recording in comparison to intracellular recording is that the activity of neurons can be recorded without having to impale and consequently damage them. There are two basic ways to conduct extracellular recording, monophasic and biphasic. Monophasic recording utilizes one electrode plus a ground electrode. The amplified signal is the voltage difference between the ground (0V) and the membrane potential recorded by the electrode attached to the nerve (approximately +70 mV outside the cell with respect to the inside). The depolarization of an action potential turns the outside negative with respect to the inside (approximately -40 to -55mV), as sodium flux in. This is represented by a downward peak on the graph.

Biphasic recording utilizes two electrodes and measures the potential difference between them. The depolarization of an action potential passes the electrodes temporally delayed. The first electrode becomes negative with respect to the second electrode (downward peak). The depolarization propagates towards the second electrode. At one point both electrodes are depolarized and the difference is zero (graph returns to zero-line), before the second electrode turns negative with respect to the first one (upward peak). The plot in Figure A.1b shows a sinusoidal shape.

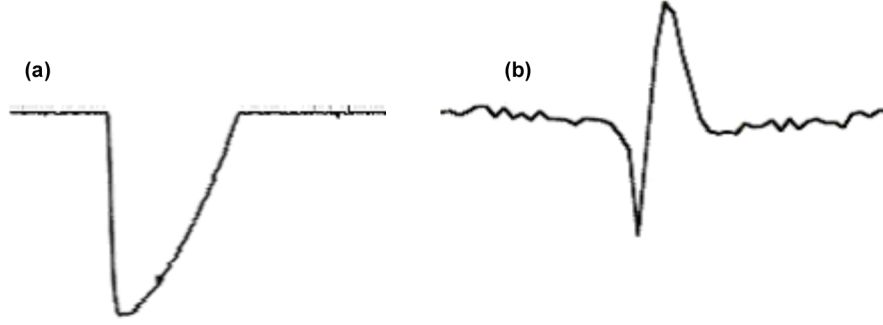


Figure A.1: Different spike shape of mono- and biphasic recording **a.** monophasic recording; plot correlates with the temporary negative charge of the outer membrane **b.** biphasic recording; plot shows the temporally delayed reversal of the membrane voltage

A.3 Spike Separation and Counting

In order to process the electrophysiological recordings taken during testing into useful information, a program was developed to determine the locations of each individual action potential event. This was accomplished by continuously taking derivatives of the data set. Once the derivative, which indicates the slope of the data, exceeded a predetermined set point, the amplitude of the data was compared to a threshold value determined by measuring the resting potential in the nerve cord. If both the derivative and threshold criteria were exceeded, the system then recorded the temporal location of the spike and proceeded to count it toward the total. Raw voltage data was also recorded to facilitate spike sorting.

As a result of the relatively large diameter electrodes used, the recording type is considered multi-unit. This means that the activity of multiple neurons is being additively recorded, which requires separation of the spikes based on the neuron they originated from. Neurons in direct contact with the electrode had a much larger voltage amplitude than neurons with indirect contact through other neurons. In addition to the difference in spike amplitudes, each neuron uses a unique spike shape to identify itself. By manually separating these characteristics, pattern tracking software could later determine the origin of each spike in the spatiotemporal pattern.

A.4 Acoustic Waveguide Design Process

The experimental setup used by previous researchers [22, 24] was reproduced. The physical design of the tube included a 12 inch long section of 6 inch nominal PVC tubing with a 1.5 inch hole drilled through the top dead center to facilitate the recording electrode being mounted on a fine

adjustment micromanipulator. A 0.5 inch diameter hole was drilled in the bottom dead center of the tube which acted as a pivot point around the magnetic base onto which the cricket was mounted. This pivot allowed the orientation of the acoustic field with respect to the specimen to be varied. The tube was cut in half and connection brackets were bonded to the PVC to act as flanges, such that the waveguide could be assembled around the preparation once positioning of the electrodes around the nerve cord was made using a vertically oriented microscope. A 6.5 inch, 8 Ω , 65W RMS, D-2K05047 speaker was mounted on each end using a 1/4 inch Lexan mounting flange. Each mounting flange was equipped with machine screw feet which allowed for leveling of the waveguide.

In order to calibrate the waveguide, frequency response analysis was performed. A 1/2" diameter Larson-Davis Model 2541 Free Field condenser microphone with a PRM900C preamp attached to a 2200C amplifier was connected to a data analysis computer. The computer was programmed to generate 10 seconds of white noise using virtual instruments (VI's) readily available in National Instruments' LabVIEW software. During the white noise excitation, microphone data was recorded with a sampling rate of 44,100 kS/s (Hz). Using the frequency response function (FRF VI) virtual instrument, the response to white noise was calculated. An ideal system would have a flat response across all frequencies. As shown in Figure A.2, the response of this configuration was not flat, but contained two distinct resonances and a chaotic response region within the frequency range of interest. Resonant peaks were clear at approximately 175 Hz and 600 Hz. In addition to the two resonant peaks present, random fluctuations in FRF amplitude from DC to 200 Hz made it clear that these frequencies could not be excited using this configuration, eliminating the use of this entire range of interest from testing. Acoustical analysis was performed using equations (2) and (4) and it was determined that the lowest resonance at 175 Hz was caused by the 1.5 inch electrode access hole in the waveguide, and that the 600Hz mode was caused by the dimensions of the cylindrical cavity. A new design was developed to eliminate these features.

In order to eliminate the electrode access hole, a new micromanipulator system was developed using a smaller Narishige C-2 adjustable clamp, which could be mounted on the same magnetic base as the cricket preparation. An adapter was fabricated out of 0.5 inch thick Lexan in order to hold the manipulator at a 45° angle with respect to the cricket mounting glass. Drawings for this

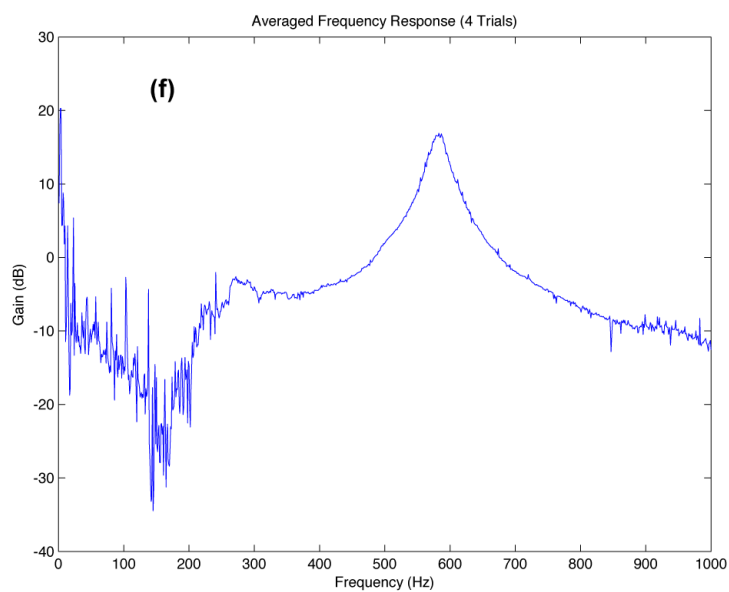


Figure A.2: Design of testing apparatus 1. **a.** dissecting microscope **b.** micromanipulator **c.** fabricated split tube design **d.** Dual hook electrode with glass armature **e.** 6.5" driver **f.** frequency response spectrum of test apparatus 1.

manipulator mount can be found in Appendix ???. A new sealed, hinged hatch design was developed to allow access for dissection without needing to disassemble the waveguide. The purpose of this feature was to eliminate the possibility of disturbing the electrode placing during the process of assembly, creating a more reliable setup. The end result was a fully sealed cylindrical waveguide shown in Figure A.3.

A.4.1 LabVIEW Work

All of the programming responsible for playing sound stimulus files as well as acquiring microphone and extracellular recording data was done using National Instruments' LabVIEW 8.6. Programming is accomplished through the use of virtual instruments (VI's) which are wired together using a visual format consistent with object oriented programming. Programs were developed for the following tasks

- perform frequency response testing of experimental setups
- Read and play WAV format sound files and record resulting neurological response

Frequency response testing is a relatively straight forward task, requiring the input signal, in this case white noise, and the response of the waveguide measured with a microphone. Pre-programmed VI's were used to compare the signals and calculate a frequency response spectrum.

Reading and playing sound files requires a much more complicated programming structure. The program was automated to read and play sequences of files by incrementing the file names, while recording and saving the extracellular recording for each. This automation allowed for the maximum number of data points to be recorded for each cricket preparation before the nerve cells died, allowing for more statistically relevant data sets. Figure A.4 gives an flow chart of the program's functionality. For a full wiring diagram of LabVIEW VI's used for this task, please see Appendix B.

A.4.2 Sound File Generation

Sound files were generated in .wav file format in order to compress the amount of disk space required for each file. MatLab programming was developed to create the sound files, each of which was responsible for isolating a particular parameter of interest, as outlined in § 3.1. A function called

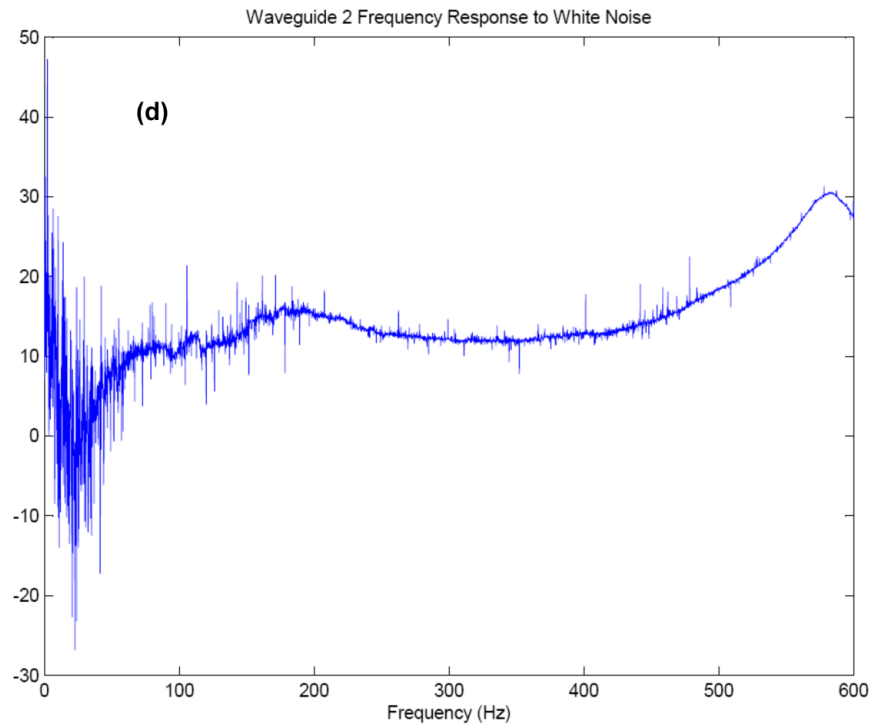
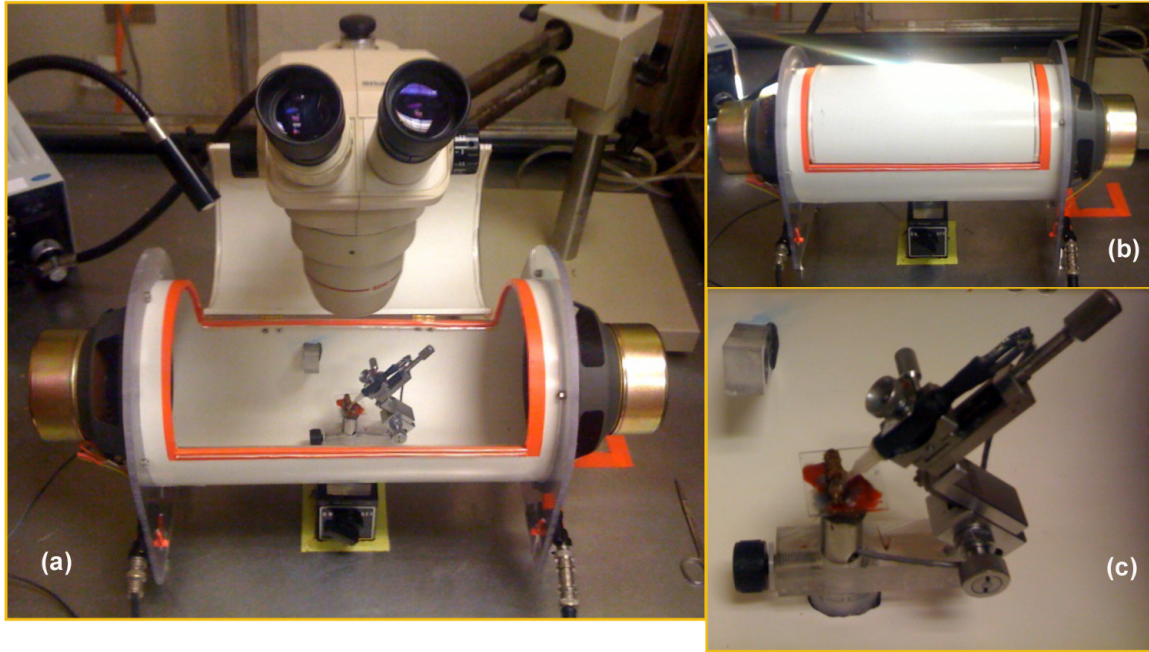


Figure A.3: Design of testing apparatus 2. **a.** Fabricated waveguide. **b.** Sealed hatch access **c.** Internal micromanipulator mount. **d.** Frequency response spectrum of test apparatus 2.

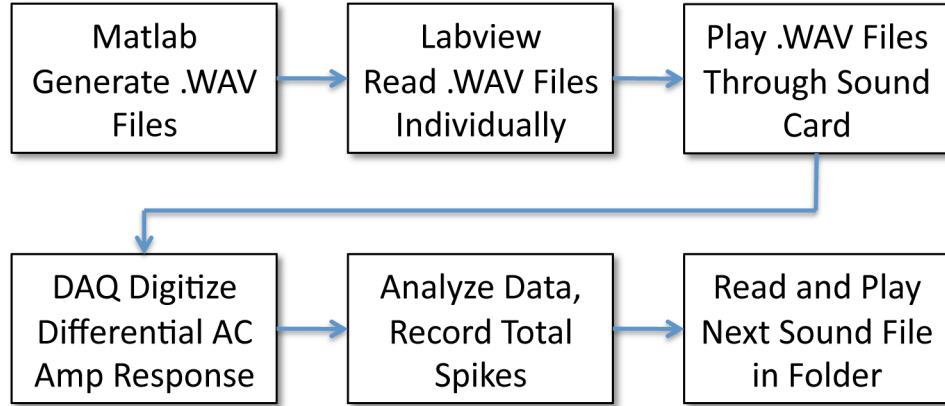


Figure A.4: Block Diagram of Program Used for Reading and Playing .WAV Files While Recording Cricket Response.

SignalGenGauss.m was programmed to develop Gaussian enveloped sine waves with a maximum amplitude of 1. Additionally, filtered white noise could also be applied to the signal with varying amplitudes. The output of this program was a single WAV file containing one stimulus signal, delayed by a specified time. An additional MatLab program, *wavecreator.m* was developed to automate file creation using a single command for each gaussian window standard deviation of interest, outputting a series of stimulus files containing the center frequencies specified by the user.

A.5 White Noise Exposure Data

The following data shows traces recorded from the cricket's extracellular electrodes during 120 second exposures to white noise with various filters. Although there is distinctly more activity in the first 20-30 seconds, which sharply drops off, the fact that it never completely habituates made white noise an unusable masking signal for testing.

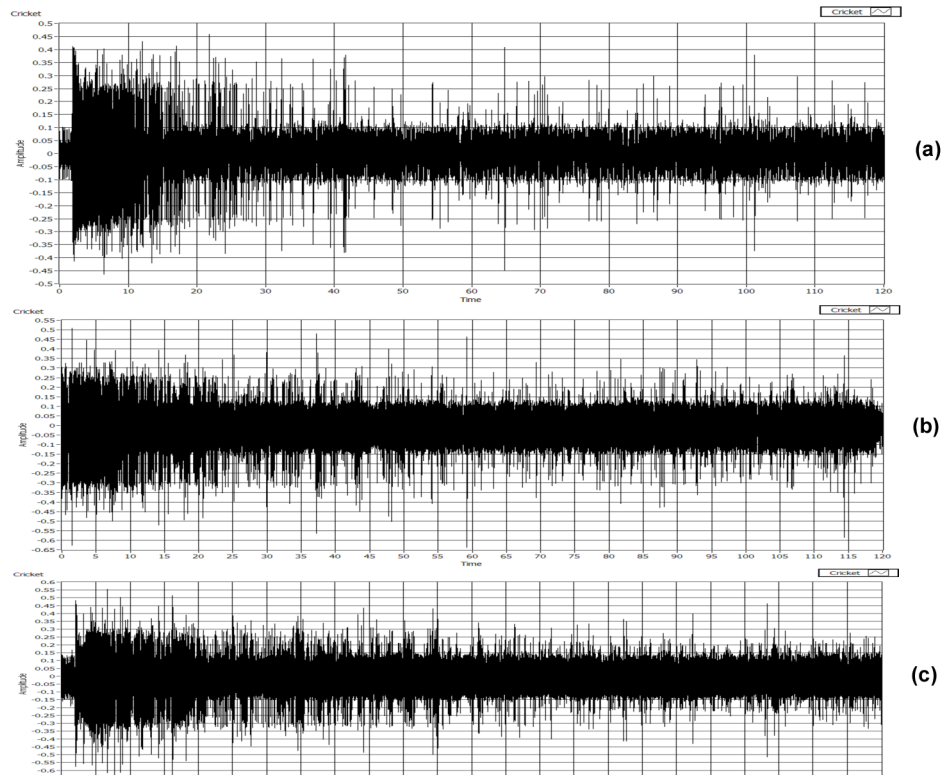


Figure A.5: 120 Second Recordings in Response to White Noise Bandpass Filtered over **a.** 20-70 Hz, **b.** 50-550Hz, **c.** Unfiltered.

LABVIEW PROGRAMMING

The following figures display the LabVIEW block diagrams for the programs used to acquire data and provide stimulus signals to the cricket. Digital copy of this code can be obtained by direct request to the author.

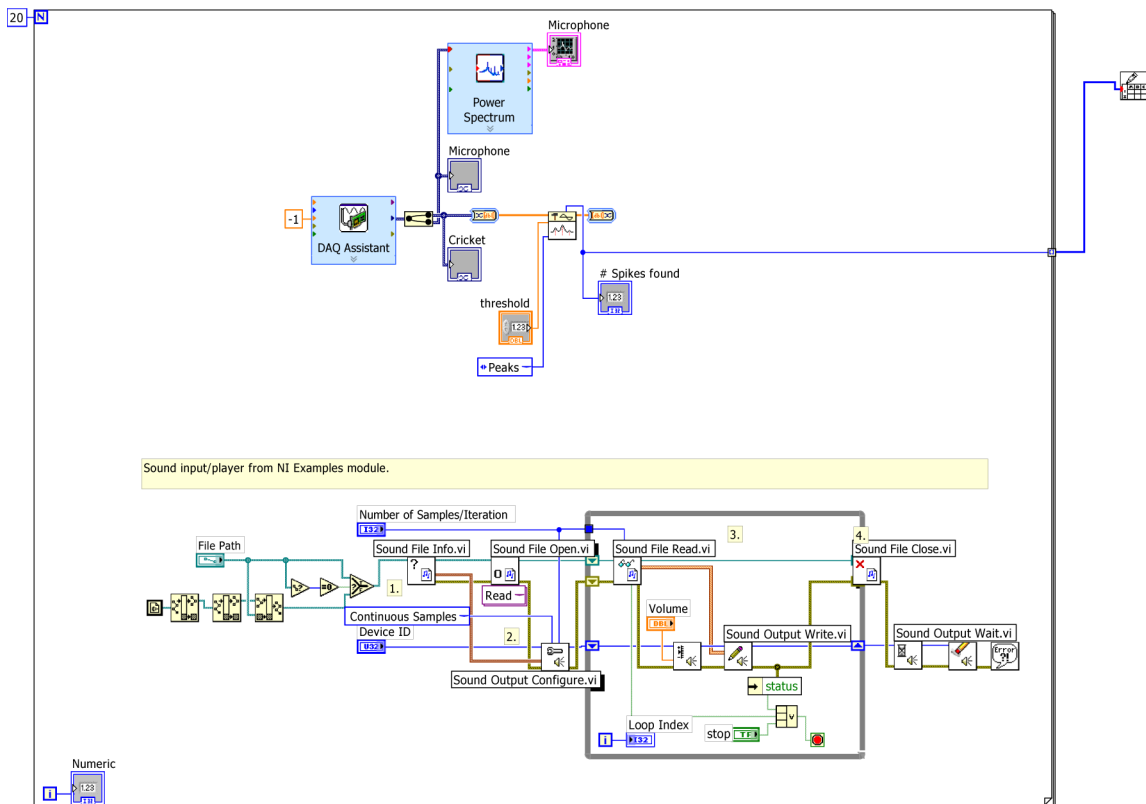


Figure B.1: Labview program for reading a single stimulus WAV file and recording cricket response

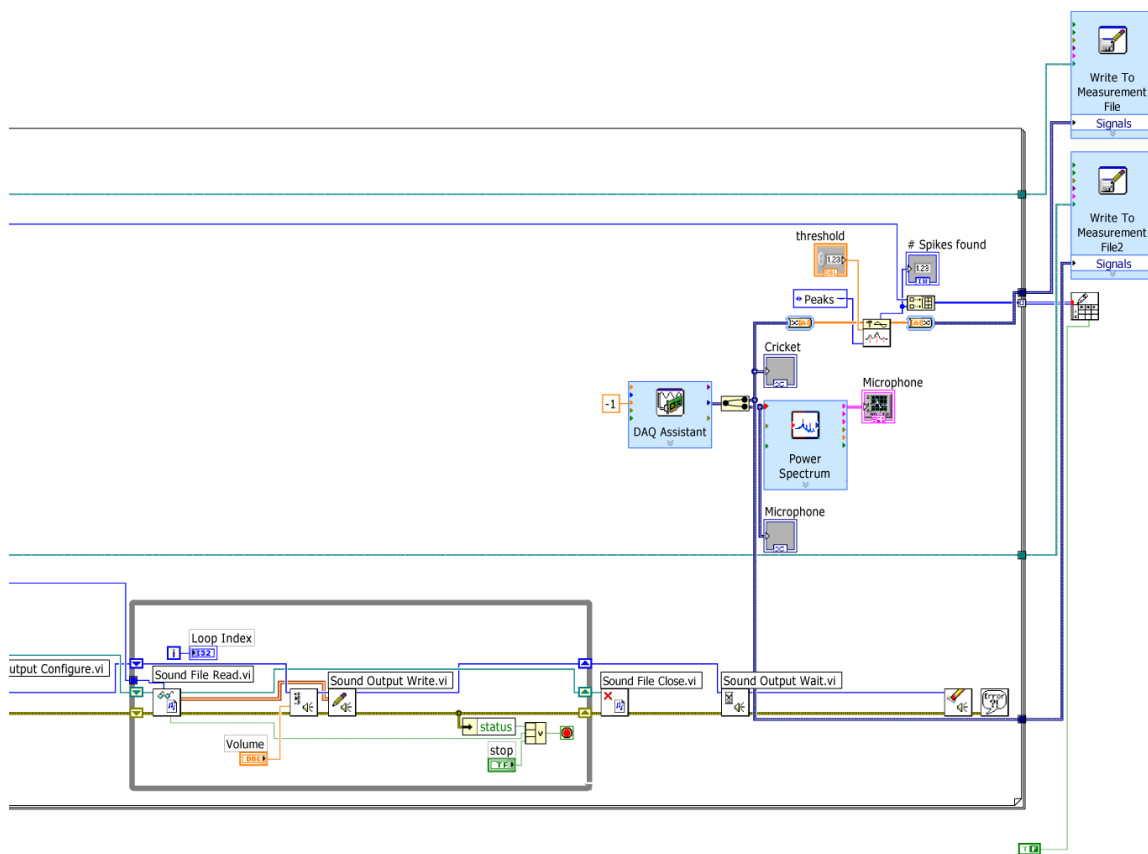


Figure B.3: Block Diagram 2 of 2 for reading and playing multiple WAV files, recording cricket response, and resolving spike temporal locations

APPENDIX C

RAW DATA

Table C.1: Raw Data: behavioral response to combined acoustic and vibration stimuli Table 1 of 2.

Frequency (Hz)	40	70	100	130
Trial #				
1	55	45	140	25
2	140	45	160	100
3	110	90	110	30
4	0	45	90	50
5	140	10	95	55
6	140	60	70	125
7	45	130	125	155
8	90	45	90	170
9	0	160	45	90
10	150	10	110	175
11	90	45	55	160
12	130	130	90	175
13	20	120	145	160
14	70	35	40	170
15	140	135	10	130
16	130	45	90	135
17	65	10	90	180
18	120	0	90	130
19	100	45	40	90
20	130	20	45	135

Table C.2: Raw Data: behavioral response to combined acoustic and vibration stimuli Table 2 of 2.

Frequency (Hz)	160	190	220	250
Trial #				
1	65	90	125	95
2	15	60	70	90
3	85	100	90	70
4	180	160	0	110
5	100	120	60	25
6	120	170	100	120
7	170	75	180	175
8	145	55	120	90
9	155	125	125	175
10	175	90	25	130
11	135	90	20	80
12	145	40	0	110
13	0	95	110	35
14	0	20	150	175
15	70	80	135	120
16	65	65	60	100
17	40	95	0	90
18	75	80	40	150
19	35	170	10	45
20	105	180	50	160

Bibliography

- [1] BABA, Y. and SHIMOZAWA, T., “Diversity of motor responses initiated by a wind stimulus in the freely moving cricket, *Gryllus bimaculatus*,” *Zoological science*, vol. 14, no. 4, pp. 587–594, 1997.
- [2] BACON, J. and MURPHEY, R., “Receptive fields of cricket giant interneurons are related to their dendritic structure,” *The Journal of Physiology*, vol. 352, no. 1, pp. 601–623, 1984.
- [3] BIALEK, W., RIEKE, F., DE RUYTER VAN STEVENINCK, R., and WARLAND, D., “Reading a neural code,” *Science*, vol. 252, no. 5014, pp. 1854–1857, 1991.
- [4] BRUNGART, D. S., *Preliminary Model of Auditory Distance Perception for Nearby Sources*. Computational Models of Auditory Function, Burke, VA: IOS Press, 2001.
- [5] DANGLES, O., MAGAL, C., PIERRE, D., OLIVIER, A., and CASAS, J., “Variation in morphology and performance of predator-sensing system in wild cricket populations,” *The Journal of Experimental Biology*, vol. 208, pp. 461–468, 2005.
- [6] DECHANT, H., RAMMERSTORFER, F., and BARTH, F., “Arthropod touch reception: stimulus transformation and finite element model of spider tactile hairs,” *Journal of Comparative Physiology A: Neuroethology, Sensory, Neural, and Behavioral Physiology*, vol. 187, no. 4, pp. 313–322, 2001.
- [7] DIJKSTRA, M., VAN BAAR, J., WIEGERINK, R., LAMMERINK, T., DE BOER, J., and KRJNEN, G., “Artificial sensory hairs based on the flow sensitive receptor hairs of crickets,” *J. Micromech. and Microeng.*, vol. 15, no. 7, pp. S132–S138, 2005.
- [8] DIMITROV, A. and MILLER, J., “Neural coding and decoding: communication channels and quantization,” *Network: Computation in Neural Systems*, vol. 12, no. 4, pp. 441–472, 2001.
- [9] D’SPAIN, G. L., LUBY, J. C., WILSON, G., and GRAMANN, R. A., “Vector sensors and vector sensor line arrays: Comments on optimal array gain and detection,” *J. Acoust. Soc. Am.*, vol. 120, pp. 171–185, 2006.
- [10] EATON, C., CROOK, S., CUMMINS, G., and JACOBS, G., “Modeling ion channels from the cricket cercal sensory system,” *Neurocomputing*, vol. 58, pp. 409–415, 2004.
- [11] EDWARDS, J. and PALKA, J., “The cerci and abdominal giant fibres of the house cricket, *acheta domesticus*. i. anatomy and physiology of normal adults,” *Proceedings of the Royal Society of London. Series B, Biological Sciences*, vol. 185, no. 1078, pp. 83–103, 1974.
- [12] ERIKSSON, L., “Higher order mode effects in circular ducts and expansion chambers,” *The Journal of the Acoustical Society of America*, vol. 68, p. 545, 1980.
- [13] FAHY, F., GARDONIO, P., and HAMBRIC, S., “Sound and Structural Vibration,” *The Journal of the Acoustical Society of America*, vol. 122, p. 689, 2007.
- [14] FAY, R., *Hearing in Vertebrates: a Psychophysics Databook*. Hill-Fay Associates, Winnetka, Ill., 1988.
- [15] FLETCHER, N., *Acoustic Systems in Biology*. Oxford University Press, USA, 1992.

- [16] GEDEON, T., PARKER, A., and DIMITROV, A., “Information distortion and neural coding,” *Canadian applied mathematics quarterly*, vol. 10, no. 1, pp. 33–70, 2003.
- [17] GOODMAN, M., “Mechanosensation,” *The C. elegans Research Community (ed) WormBook*, doi/10.1895/wormbook, vol. 1, no. 1, p. 14, 2006.
- [18] HEYS, J., GEDEON, T., KNOTT, B., and KIM, Y., “Modeling arthropod filiform hair motion using the penalty immersed boundary method,” *Journal of Biomechanics*, 2008.
- [19] HUBER, F., MOORE, T., and LOHER, W., *Cricket Behavior and Neurobiology*. Cornell University Press, 1989.
- [20] HUMPHREY, J., DEVARAKONDA, R., IGLESIAS, I., and BARTH, F., “Dynamics of arthropod filiform hairs. I. mathematical modelling of the hair and air motions,” *Philosophical Transactions of the Royal Society B: Biological Sciences*, vol. 340, no. 1294, pp. 423–444, 1993.
- [21] IZADI, N., JAGANATHARAJA, R., FLORIS, J., and KRIJNEN, G., “Optimization of cricket-inspired, biomimetic artificial hair sensors for flow sensing,” *Arxiv preprint arXiv:0802.3768*, 2008.
- [22] JACOBS, G., MILLER, J., and ALDWORTH, Z., “Computational mechanisms of mechanosensory processing in the cricket,” *Journal of Experimental Biology*, vol. 211, no. 11, p. 1819, 2008.
- [23] JAGANATHARAJA, R., IZADI, N., FLORIS, J., LAMMERINK, T., WIEGERINK, R., and KRIJNEN, G., “Model-based optimization and adaptivity of cricket-inspired biomimetic artificial hair sensor arrays,” *MicroMechanics Europe Workshop*, pp. 16–18, 2007.
- [24] KÄMPER, G. and VEDENINA, V., “Frequency-intensity characteristics of cricket cercal interneurons: units with high-pass functions,” *Journal of Comparative Physiology A: Sensory, Neural, and Behavioral Physiology*, vol. 182, no. 6, pp. 715–724, 1998.
- [25] KINSLER, L., FREY, A., COPPENS, A., and SANDERS, J., *Fundamentals of Acoustics*. Wiley, 1999.
- [26] LAURENT, G. and DAVIDOWITZ, H., “Encoding of olfactory information with oscillating neural assemblies,” *Science*, vol. 265, no. 5180, p. 1872, 1994.
- [27] LEVIN, J. and MILLER, J., “Broadband neural encoding in the cricket cercal sensory system enhanced by stochastic resonance,” *Nature*, vol. 380, no. 6570, pp. 165–168, 1996.
- [28] MAGAL, C., DANGLES, O., CAPARROY, P., and CASAS, J., “Hair canopy of cricket sensory system tuned to predator signals,” *Journal of Theoretical Biology*, vol. 241, no. 3, pp. 459–466, 2006.
- [29] OGAWA, H., CUMMINS, G., JACOBS, G., and MILLER, J., “Visualization of ensemble activity patterns of mechanosensory afferents in the cricket cercal sensory system with calcium imaging,” *J. Neurobiology*, vol. 66, no. 3, p. 293, 2006.
- [30] PALKA, J. and SCHUBIGER, M., “Central connections of receptors on rotated and exchanged cerci of crickets,” *Proceedings of the National Academy of Sciences*, vol. 72, no. 3, pp. 966–969, 1975.

- [31] PAYDAR, S., DOAN, C., and JACOBS, G., “Neural mapping of direction and frequency in the cricket cercal sensory system,” *Journal of Neuroscience*, vol. 19, no. 5, pp. 1771–1781, 1999.
- [32] PIERCE, A., *Acoustics: An Introduction to Its Physical Principles and Applications*. New York: Acoust. Soc. of America, 1989.
- [33] QI, H., WANG, X., IYENGAR, S., and CHAKRABARTY, K., “Multisensor data fusion in distributed sensor networks using mobile agents,” in *Information Fusion 2001*, p. 1116, 2001. Proceedings of the International Conference on Information Fusion.
- [34] REISSMAN, T., CRAWFORD, J., and GARCIA, E., “Insect cyborgs: a new frontier in flight control systems,” in *Active and Passive Smart Structures and Integrated Systems 2007*, vol. 6525, p. 65250N, SPIE, 2007. Proceedings of SPIE.
- [35] REISSMAN, T. and GARCIA, E., “Cyborg mavs using power harvesting and behavioral control schemes,” *Advances in Science & Technology*, vol. 58, p. 5, 2008.
- [36] REISSMAN, T. and GARCIA, E., “Surgically implanted energy harvesting devices for renewable power sources in insect cyborgs,” in *ASME International Mechanical Engineering Congress and Exposition*, vol. IMECE2008, (Boston, MA), p. 9, ASME, 2008.
- [37] REISSMAN, T. and GARCIA, E., “An ultra-lightweight multi-source power harvesting system for insect cyborg sentinels,” in *ASME Conference on Smart Materials, Adaptive Structures and Intelligent Systems*, (Ellicott City, MD), p. 8, 2008.
- [38] REISSMAN, T., MACCURDY, R. B., and GARCIA, E., “Experimental study of the mechanics of motion of flapping insect flight under weight loading,” in *ASME Conference on Smart Materials, Adaptive Structures and Intelligent Systems*, (Ellicott City, MD), p. 11, 2008.
- [39] SAKAGUCHI, D. and MURPHEY, R., “The equilibrium detecting system of the cricket: physiology and morphology of an identified interneuron,” *Journal of Comparative Physiology A: Neuroethology, Sensory, Neural, and Behavioral Physiology*, vol. 150, no. 2, pp. 141–152, 1983.
- [40] SHANNON, C., “Memory requirements in a telephone exchange,” *Bell System Technical Journal*, vol. 29, pp. 343–349, 1950.
- [41] SHIMOZAWA, T., KUMAGAI, T., and BABA, Y., “Structural scaling and functional design of the cercal wind-receptor hairs of cricket,” *Journal of Comparative Physiology A: Sensory, Neural, and Behavioral Physiology*, vol. 183, no. 2, pp. 171–186, 1998.
- [42] THEUNISSEN, F., DAVID, S., SINGH, N., HSU, A., VINJE, W., and GALLANT, J., “Estimating spatio-temporal receptive fields of auditory and visual neurons from their responses to natural stimuli,” *Network: Computation in Neural Systems*, vol. 12, no. 3, pp. 289–316, 2001.
- [43] THEUNISSEN, F. and MILLER, J., “Representation of sensory information in the cricket cercal sensory system. II. Information theoretic calculation of system accuracy and optimal tuning-curve widths of four primary interneurons,” *Journal of neurophysiology*, vol. 66, no. 5, p. 1690, 1991.
- [44] VAN TREES, H. L., *Detection, Estimation, and Modulation Theory, Part IV, Optimum Array Processing*. New York: Wiley, 2002.

- [45] WEHR, M. and LAURENT, G., “Odour encoding by temporal sequences of firing in oscillating neural assemblies,” *Nature*, vol. 384, no. 6605, pp. 162–166, 1996.
- [46] WIESE, K., “Influence of vibration on cricket hearing: Interaction of low frequency vibration and acoustic stimuli in the omega neuron,” *Journal of Comparative Physiology A: Neuroethology, Sensory, Neural, and Behavioral Physiology*, vol. 143, no. 1, pp. 135–142, 1981.
- [47] YOUNG, D. and AUSTIN, T., “Vibration of Rectangular Plates by Ritz Method,” *Vibration: Beams, Plates, and Shells*, p. 68, 1976.